

Research Article

Karolina Pantazatou*, Kristoffer Mattisson, Per-Ola Olsson, Erik Telldén, Anders Kettisen, Soraya Hosseinvash Azari, Wenjing Liu, Lars Harrie

Influence of land cover on noise simulation output – A case study in Malmö, Sweden

<https://doi.org/10.1515/noise-2025-0016>

received November 18, 2024; accepted February 06, 2025

Abstract: Determining the land cover (LC) data requirements used as input to noise simulations is essential for planning sustainable urban densifications. This study examines how different LC datasets influence simulated environmental noise levels of road traffic using Nord2000 in an urban area of 1 km² in southern Sweden. Four LC datasets were used. The first dataset was based on satellite data (spatial resolution 10 m) combined with various other datasets implementing an LC classification algorithm prioritizing vegetation. The second dataset was created by applying an LC majority priority rule over every cell of the first dataset. The third dataset was produced by applying a convolutional neural network over an orthophoto (0.08 m spatial resolution), while the fourth dataset was created by manually digitizing ground surfaces over the same orthophoto also utilizing data from the municipality's basemap. The results show that LC data impact simulated noise levels, with priority rules in LC classification algorithms having a greater effect than spatial resolution. Statistically significant differences (up to 3 dB(A)) were found when comparing the simulated noise levels generated using the vegetation-prioritizing LC dataset compared to the simulated noise levels of the other LC datasets.

Keywords: noise simulations, Nord2000, convolutional neural networks, land cover, semantic 3D city models, sustainable urban planning

1 Introduction

Urban densifications are becoming increasingly more common as a result of the dual effect of global population growth [1] and urbanization [2]. Urban densifications are considered more sustainable compared to urban sprawls [3], since more people get to use the same infrastructure while valuable agricultural land, often found on the outskirts of cities, is preserved [4]. However, planning an urban densification is a complex task, with one of the major challenges being the mitigation of noise pollution [5,6].

Long-term exposure to noise has been associated with sleep disturbance [7], cardiovascular disease [8,9], metabolic disease [8], stress [10], depression [11], annoyance [12], as well as reduced cognitive performance [13,14] and productivity in the workplace [15]. In the EU, there are estimations of about 12,000 people dying prematurely every year due to exposure to environmental noise, with road traffic as the main source [16]. Noise has also been identified as the causal effect behind changes in the physiology (e.g. reduced reproductive success and increased mortality) and behaviour (temporary or permanent departure from noisy areas) of urban wildlife, thus threatening the biodiversity and balance of urban ecosystems [16,17].

To prevent negative health impacts, the United Nations' World Health Organization (WHO) and European Union (EU) have issued noise guidelines while individual countries have introduced noise-regulating laws and recommendations. Since road traffic is the most widespread noise source in Europe and the main contributor to high-level noise exposure in urban populations [18], WHO's guidelines recommend a reduction of road traffic noise levels below 53 dB(A)¹ for the entire day L_{den}^2 and below 45 dB(A) for night-

* **Corresponding author: Karolina Pantazatou**, Department of Physical Geography and Ecosystem Science, Lund University, Lund, Sweden, e-mail: karolina.pantazatou@nateko.lu.se

Kristoffer Mattisson: Division of Occupational and Environmental Medicine, Lund University, Lund, Sweden

Per-Ola Olsson, Soraya Hosseinvash Azari, Wenjing Liu, Lars Harrie: Department of Physical Geography and Ecosystem Science, Lund University, Lund, Sweden

Erik Telldén, Anders Kettisen: Department of Science and Technology (ITN), Linköping University, Norrköping, Sweden

1 A-weighted decibel dB(A) is an expression of the relative loudness of sounds as perceived by the human ear.

2 L_{den} is a noise metric (expressed in dB(A)) used to reflect a person's cumulative exposure to sound over a 24 h period (day, evening, night) with a penalty of 5 dB(A) added for the evening hours, and a penalty of 10 dB(A) added for the nighttime hours.

time L_{night} ³ [19]. EU has issued the European Noise Directive (END) to monitor and address the exposure of citizens to noise pollution. According to END, municipalities (population > 100,000 inhabitants) of every member state are obliged to create and publish noise maps as well as noise management action plans in 5-year intervals for locations with estimated noise levels above 55 dB(A) L_{den} and 50 dB(A) L_{night} [20]. In Sweden, it is mandatory to check for noise pollution when planning new buildings [21–24]. This is controlled at various stages of the urban planning process (*e.g.* detailed development plan, building permit).

Exposure to noise pollution is assessed by performing regular real-world noise measurements or by conducting computer-based noise simulations. Computer-based noise simulations are less expensive and have the potential to cover larger geographic areas compared to high-quality noise measurements [25]. Consequently, noise analyses required by the EU or for urban planning purposes are usually conducted by executing noise simulations [26,27].

However, noise simulations are time-consuming, and the increasing pressure of constructing residential buildings more rapidly in Sweden has led to initiatives aiming to repeal the laws and cancel the recommendations related to noise pollution in urban planning [28,29]. Albeit, in the context of urban densifications, even if modern sound-insulating techniques could potentially largely prevent outdoor noise from entering buildings [30,31], this still leaves the issue of population and wildlife exposure to noise in outdoor areas open. Hence, excluding noise analyses from the planning of urban densifications would jeopardize urban sustainability. To avoid that, it is imperative to reduce the time required for conducting noise analyses. Common factors responsible for the prolonged duration of noise analyses (besides available computational power) are (1) the size of the study area, (2) the level of detail of the input datasets, (3) the time required for finding and pre-processing input datasets, and (4) the choice of noise propagation model (NPM) [32].

Noise simulations are based on a NPM, which is a mathematical model describing the physical processes that disperse noise emitted by a source in space and time. By using the NPM, it is possible to estimate how noise propagates from one or several sources to target points (receivers) often placed on building façades. Several NPMs have been developed. The END recommends the implementation of the CNOSSOS-EU NPM [33] when conducting city-scale (1–5,000 km²) noise analyses. Currently, in Sweden, it is mandatory to execute noise

simulations for urban planning using the RTN-96 NPM. RTN-96 is soon to be replaced by Nord2000. Nord2000 is more detailed compared to CNOSSOS-EU and RTN-96 [34–38] and is, therefore, deemed more suitable for simulating noise propagation on local or street scale (1 m² to 1 km²) for, *e.g.* urban planning.

Nord2000 requires information on the characteristics (geometry and material) of ground surfaces (vegetation, soil, rock, *etc.*) and man-made objects (buildings, roads, *etc.*) including their flow resistivity (reflecting the air permeability through porous materials), which is related, among others, to the specific acoustic impedance and whose units are N s/m⁴ or Pa s/m². Specific Acoustic Impedance (Z) is defined as the complex ratio of the effective sound pressure at a point of an acoustic medium to the effective particle velocity at that point and is measured in units of N s/m³. Land cover (LC) information describes the material of a ground surface (*e.g.* grass) and is not to be confused with land use (LU), which refers to how a ground surface is utilized (*e.g.* park or football court). Nord2000 uses LC information to identify the noise absorbance of different ground surfaces and man-made objects [39]. LC information is available in varying formats (raster, vector) and quality, but producing it is a non-trivial, time-demanding task often requiring the processing of multiple datasets from different sources [40].

CORINE is a pan-European open-access LC/LU product featuring 44 thematic classes with a 6-yearly updating frequency, a minimum mapping unit of 25 ha for aerial phenomena and a minimum width of 100 m for linear phenomena [41]. The European Environment Agency (EEA) in collaboration with Copernicus EU and the European Space Agency have created the Urban Atlas, an open-access product that includes LC information on a selected number of urban areas in Europe [42]. The Urban Atlas LC information is updated every 6 years and has a spatial resolution of 10 m [42]. Many countries also provide open-access LC datasets with national coverage, usually derived from satellite remote sensing data of a higher spatial resolution than CORINE [40,41,43]. Municipalities collect information on how urban ground surfaces are utilized as a primary resource for urban planning. This information is produced by processing aerial images, very-high-resolution satellite images [44], LiDAR data [45], and sometimes even terrestrial observations. The final output dataset is stored in vector format (lines) and is characterized by high spatial accuracy. Though the (LC-related) dataset is frequently updated, producing surfaces (polygons) from line layers is a complex and time-consuming task.

Cities often have very detailed LC data for some LC classes such as transportation, water, and park areas, but their data seldomly cover the whole city. A possible solution for producing complete LC datasets for cities is to

³ L_{night} is a noise metric (expressed in dB(A)) used to reflect a person's exposure to sound during nighttime.

utilize artificial intelligence (AI) techniques such as convolutional neural networks (CNN). CNNs can be used to automatically derive LC information from aerial and satellite images [46–53]. CNNs are the cornerstone of most semantic segmentation models (*i.e.* a computer vision task in which the goal is to categorize each pixel in an image into a class or object), due to their ability to learn spatial hierarchies and capture localized patterns [54]. Though aerial and satellite imagery are openly available from multiple sources, this is not the case for LC training datasets. Some international initiatives exist for LC classification, but the number of available datasets for training and evaluation is still significantly lower compared to other domains (*e.g.* autonomous driving) [55,56].

To minimize the preprocessing time of LC input data to noise simulations, it is important to automate the mapping of flow resistivity value to every LC class. There are examples of such mappings [57,58,39,59,60], but whilst there is no LC classification standard detailed enough for urban areas, additional work is often required [61].

Semantic 3D city models could be utilised to minimize the time required for finding and accessing input datasets for noise simulations. Semantic 3D city models are digital 3D representations of the urban physical environment including the option to store semantic information for every geometry (building address, material of building façade, *etc.*) [62]. The open geospatial consortium has released a semantic 3D city model standard called CityGML [63,64]. CityGML includes several themes (*Building, Transportation, City Furniture, Vegetation, LandUse, etc.*) supporting the storage of LC data and other input data to NPM. Furthermore, CityGML can be extended to support the storage of additional information required by certain applications using application domain extensions (ADE) [63]. *Noise ADE* is an example of a CityGML ADE created to support noise simulations including acoustic impedance value per ground surface object [65].

As noted above, the most common factors responsible for the prolonged duration of noise analyses are the size of the study area, the input data level of detail, the time required for finding and pre-processing input data, and the choice of NPM. From an urban densification planning perspective, the size of the study area is preset to local or street-level while the choice of NPM has already been pre-determined by national directives, leaving only the two remaining factors open to interpretation. Here the focus is set on LC. LC datasets have the potential to become accessible to users by being stored in the *LandUse* theme of semantic 3D city models. However, it is crucial to determine the minimum requirements an LC layer must meet to be suitable as input to noise simulations before storing it in that manner. As previously mentioned, LC data varies depending on spatial resolution, temporal updating frequency as well

as on the observation data and classification system used to produce it. Another factor affecting the suitability of raster LC datasets in noise simulation analyses is the priority rules applied. For example, for raster cells containing more than one LC class, a majority rule could be applied; alternatively, the LC class could be set based on LC class priority. The aim of this study is to examine the effect of different LC input data on noise simulations. The following research questions are addressed:

- Is noise simulation output affected by different priority rules applied to produce an LC dataset?
- What is the influence of the LC data spatial resolution on noise simulation output?
- From a noise simulation perspective, what should the specification requirements for the LC classification system producing LC datasets be?

2 Methods

This section is dedicated to presenting the study area along with the materials and methods used for the implementation of our case studies. It should be mentioned that all case studies consider car traffic as the only noise source.

2.1 Study area

The study area encompasses the new Bellevue and Lorensborg neighbourhoods of Malmö municipality in southern Sweden and covers an area of approximately 945,000 m² (Figure 1). The location was chosen because it was recently deemed suitable for densification. The area is dominated by residential buildings (villas as well as 3–6 story high buildings) with some commercial and educational buildings also being present. Moreover, the study area is characterized by varying land cover comprising both vegetated areas (parks, gardens, traffic islands, *etc.*) and various built-up surfaces (roads, pavements, car parks, cycle paths, walking paths, sports facilities, school yards, refuge islands, pools, ponds, *etc.*) close to the city centre.

The area includes some urban roads that are highly trafficked (Figure 2) with the highest loads being observed on Lorensborgsgatan, Stadiongatan, and Ärtholmsvägen (marked in orange and red colours correspondingly). These roads are used for transportation in and out of the city centre.

Figure 1 highlights the buildings that were used as input to the noise simulations in red and white colours. The red buildings represent the buildings hosting receivers, while all buildings (white and red) function as

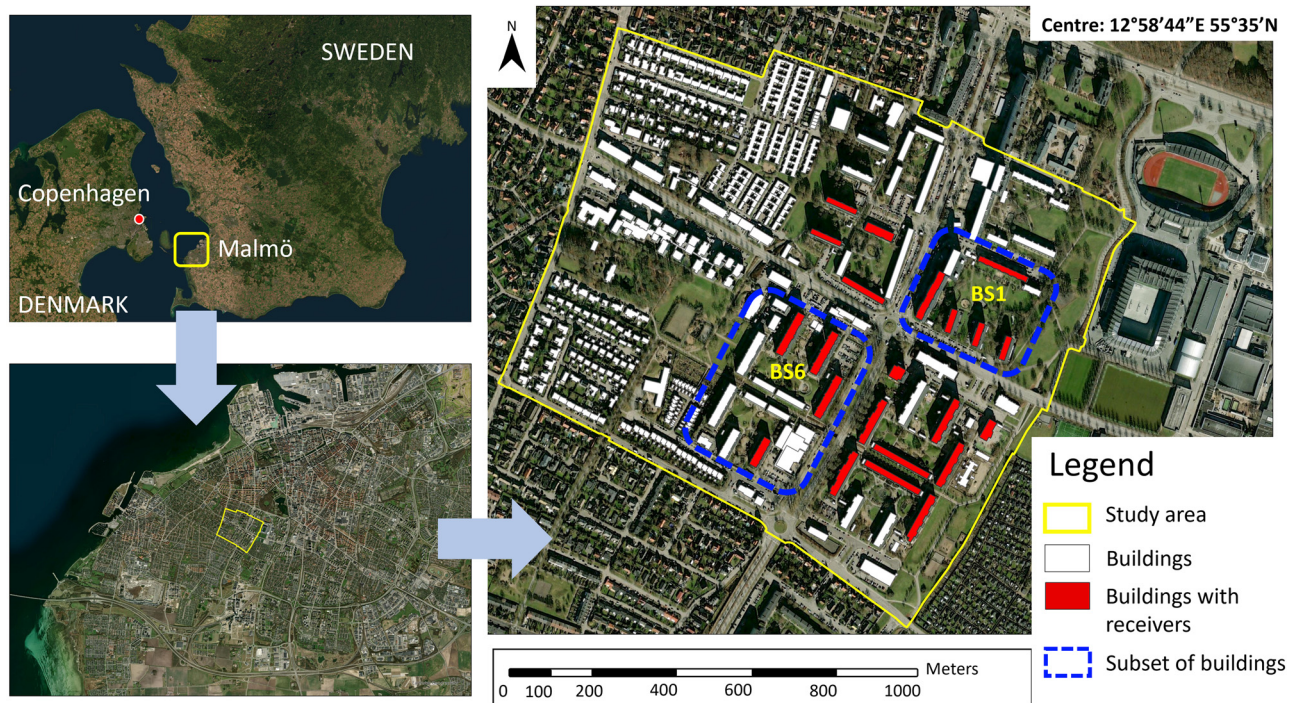


Figure 1: Study area – Lorensborg and new Bellevue neighbourhoods in Malmö municipality, southern Sweden.

noise-obstructing surfaces. In the context of this study, receivers are defined as point locations placed at a certain height above ground (1.5 and 4.0 m) and at 0.1 m distance from the building façade for registering the noise levels computed by the noise simulation software. The red buildings were chosen based on how close they were to highly trafficked parts of urban roads (sound source), how varying the land cover between the sound source and the building in questions was, the building typology (shape and height) as well as the use of the building (residential, commercial, educational, retirement home, *etc.*).

Trial simulations for all LC layers were performed using receivers from a subset of the study area (*i.e.* buildings identified in BS1 in Figure 1), positioned at heights of 1.5 and 4.0 m above ground (recommended receiver heights by Kragh *et al.* [39] and Kephelopoulou *et al.* [33]). As the largest differences in dB(A) L_{den} were observed for receivers placed 1.5 m above ground, we decided to execute noise simulations for the remaining buildings only at that height. An additional reason for this was that the recommended receiver height for sensing noise pollution for one-storey buildings was 1.5 m [39] and that we wanted to explore the worst-case noise exposure scenario for day-care centres, schools, retirement homes, residential apartments, and offices located on the ground floor. When comparing the noise simulation outputs with different LC layers as inputs, the most noticeable differences are observed for receivers located on buildings in BS6 (Figure 1).

2.2 Land cover data

Four LC datasets were used in this study (described in detail in Sections 2.2.1–2.2.4):

- **NMDa** (NMD-automatic was produced by reclassifying NMD⁴ LC data to NS-LC).
- **NMDm** (NMD-manual was produced by manually implementing an LC majority rule per NMD pixel).
- **AIO** (AI-orthophoto was produced by applying a CNN-based image classification over an orthophoto).
- **PKO** (Basemap-orthophoto (Swedish: *Primärkarta-Ortofoto*) was produced by manually digitizing LC polygons from municipal basemap line vectors placed on top of an orthophoto).

All datasets adopt the same LC classification system described in a preliminary version of the new *national specifications on LC* (here denoted as NS-LC) that are currently under review by the Swedish Mapping, Cadastral and Land Registration Authority (*Lantmäteriet*). NS-LC covers six main LC themes: *forest*, *built-up surfaces*, *open wetland*, *open solid ground*, *tundra*, and *water*. The themes that are most relevant for urban areas are *forest*, *built-up surfaces*, *open solid ground*, and (potentially) *water*. Additionally, NS-LC presents

⁴ NMD: Swedish National Land Cover Database (*Nationella Marktäckedata*).

information on the themes at four different levels of detail (L1–L4). Originally, the LC datasets were available at different NS-LC levels of detail (NMDa: NS-LC L2, NMDm: NS-LC L4, AIO: NS-LC L2, and PKO: NS-LC L4). Though all noise simulations were executed using LC datasets at the highest level of detail they were available in, in Section 3.1, all four LC datasets have been reclassified to NS-LC L2 to be comparable. For more information on the NS-LC themes and their corresponding levels of detail, check Tables A1–A3.

It was decided to distinguish on-ground from above-ground vegetation. Hence, the forest LC thematic classes have been reclassified to depict the actual material of the corresponding ground surface. Above-ground vegetation (trees, bushes, etc.) can be represented by 3D objects (e.g. *SolitaryVegetationObject* or *PlantCover* in CityGML's vegetation theme [63]) and imported to noise simulation software [66]. Then, the noise shielding capacity of the 3D vegetation objects can be set separately depending on their species. As the focus of this study has been to examine the effects of ground surfaces from different LC datasets, 3D representations of trees were not considered.

The LC datasets have received a flow resistivity value for every object (cell or polygon) depending on their corresponding NS-LC class (Table A4).

2.2.1 Reclassified national LC data (NMDa)

The first LC dataset, from now on referred to as *NMDa*, is based on the national LC dataset (NMD) from the Swedish National Environmental Protection Agency (*Naturvårdsverket*). *Naturvårdsverket* has undertaken the task of producing and disseminating an LC dataset of 10 m spatial resolution with national coverage, every 5 years, as open data. Though the dataset is primarily based on satellite images from Sentinel-2, it is actually a combination of geodata from several Swedish agencies and organizations, including *Lantmäteriet*, the Swedish Board of Agriculture (*Jordbruksverket*), the Swedish Forest Agency (*Skogsstyrelsen*), Statistics Sweden (SCB), the Swedish Transport Administration (*Trafikverket*), and others [67].

NMD data are produced based on a set of priority rules specified by [67], which are summarized below. For raster



Figure 2: Map displaying road traffic density as the average number of vehicles per day for 2020 (Malmö municipality, 2020).

cells where vegetation is present, the vegetation is prioritized over any other LC class except for main roads and buildings. Regarding main roads, there is the restriction that they must be represented by a continuous line of adjacent raster cells. Concerning buildings, the general rule is that a raster cell is classified as “building” only if its centroid is covered by the building footprint (data acquired from Lantmäteriet). Manmade water sources (pond, dam, canal, reservoir, etc.) are only represented if they cover an area greater than 100 m² [43]. Consequently, water-covered urban areas such as ponds or swimming pools are rarely represented in NMD.

The original NMD data covering the study area was vectorized and automatically reclassified to NS-LC using a Python script. A matrix was used to map the NMD LC thematic classes to the corresponding NS-LC thematic classes (conversion matrix shown in Table A5). The mapping was examined and approved by noise experts (M. Ögren, University of Gothenburg, Sahlgrenska Academy, Occupational and Environmental Medicine, Gothenburg & A. Gustafson The Swedish National Road and Transportation Research Institute, Gothenburg, personal communication, August 13, 2023).

2.2.2 Manually improved LC data from NMD (NMDm)

The second LC dataset, from now on referred to as *NMDm*, is produced by overlaying a transparent version of the NMDa dataset over an orthophoto (source: Malmö municipality, spatial resolution: 0.08 m, year: 2018), visually inspecting the content of every cell, applying the majority rule (*i.e.* determining the LC class that covers the largest area of the cell), and changing the LC classification of a cell when the result of the majority rule does not coincide with the already registered LC class. Ground photos taken by the authors from parts of the study area that are currently under development (inner yards of buildings at Stensjögatan 50, Hålsjögatan 5, Delsjögatan 2, and Svansjögatan 39) were utilized along with Google Earth and Google Street View imagery to determine the actual ground surface material in places where this was hard to conclude just by viewing the orthophoto. The dataset has a spatial resolution of 10 m.

2.2.3 AI-generated LC (AIO)

The third LC dataset, from now on referred to as *AIO*, was the result of a CNN processing the Malmö municipality orthophoto. A CNN processes an image by passing it through multiple layers of filters. Each layer progressively detects different features, starting with basic elements like edges and advancing to more complex patterns (*e.g.* objects or structures). This

enables CNNs to recognize and categorize elements within an image.

In this study, we employed a combination of the open libraries DeepLabV3 [68] and ResNet-50 architectures [69] to strike a balance between accuracy and computational efficiency. ResNet-50 acts as the feature extractor, capturing various levels of spatial information, while DeepLabV3 enhances this by using atrous (dilated) convolutions to capture multi-scale contextual information without losing resolution, which is critical for segmenting fine details. Additionally, the network uses an Atrous Spatial Pyramid Pooling (ASPP) module that applies atrous convolutions at multiple rates to aggregate features across different scales. This method helps capture both broader contextual information and finer image details. The output is then upsampled using bilinear interpolation to match the original image size, resulting in the final segmentation map.

The model training process involves a pixel-wise cross-entropy loss function, along with regularization techniques and batch normalization to prevent overfitting. During inference, the trained model can segment new images, classifying every pixel with high accuracy. Data augmentation techniques (*e.g.* rotation, flipping, and scaling) are applied to improve generalization. The first step in training is to collect labelled images where each pixel is annotated with a class. In this case, mask images corresponding to the training images are used. Pixel values represent class labels. These mask images are generated using GIS software (*e.g.* QGIS). Both existing and custom-created vector data (geo-located class information) are used to export raster masks. Training image data is similarly exported to rasters from the study area and its surrounding regions. The data is tiled into smaller segments for easier processing. Every class type is trained with a separate model, which is then used to classify the study area. After classification, the results are imported into QGIS as raster layers, which are vectorized to generate polygons. The layers are further processed to handle overlaps where multiple models classify the same area differently. A hierarchical structure is used to resolve conflicts, prioritizing classes with more training data. The hierarchy is as follows: (1) roads, (2) buildings, (3) vegetation, and (4) other built-up surfaces.

Regions not classified by any model are modelled as “other built-up surfaces.” Water was not modelled due to limited cases of such examples in the training dataset. Only swimming pools were present in the training dataset and most of them were covered not exposing the water surface.

The AI-generated LC dataset included some holes (objects: 7,121, area: 60 m²) and several very small LC objects each covering an area <1 m² (objects: 1,600, area: 486.6 m²). In total, the area covered by both problematic cases corresponded to

6% of the study area. To execute the noise simulations and reduce the execution time, the holes were covered and merged with the neighbouring LC object they shared the longest border with. LC objects representing buildings or roads were excluded from this process as it was deemed important for them to maintain their original shape and area. The same approach was followed when eliminating all small LC objects (area <1 m²).

2.2.4 LC data based on municipality base maps and orthophotos (PKO)

The fourth dataset, referred to as *PKO*, was created by digitizing the municipality's base map to create polygons from all line-objects (representing property units, roads, pavements, parks, etc.). Major road polygons (2D) for a subset of the study area were not digitized but derived from Malmö municipality's 3CIM test area [70]. 3CIM is a CityGML-based national profile, currently in development under the initiative of the three largest Swedish municipalities (Stockholm, Gothenburg, and Malmö) and Lund University [70]. Road information for the remaining areas was digitized based on the municipality's base map line-objects and orthophoto. The digitized LC layer was further improved utilizing information from ground photos as well as Google Earth and Google Street View imagery to achieve an NS-LC L4 classification level. *PKO* is the most detailed of the four LC datasets; however, the process of producing it is labour intensive and time-consuming. Additionally, the different updating frequencies of the orthophoto (biannual) and the base map (continuous) complicate the process even further. In this case, the datasets containing the most recent information (i.e. ground photos and base map) were prioritized.

2.3 Other input data to noise simulations

To get a detailed representation of the ground surface, we imported elevation points from a *Digital Elevation Model DEM* (downloaded from Lantmäteriet) at a high spatial resolution (1 m).

Line vector geometries for *roads* were provided by Malmö municipality's division for property and roadwork

administration (*Fastighet och Gatukontoret – FGK*), while traffic count information (i.e. total number of vehicles per vehicle category per lane per day) for every road segment for 2020 was provided by different sources (Swedish Transport Administration (*Trafikverket*), FGK, and Malmö municipality's division for environmental administration (*Miljöförvaltningen – MF*)). The speed for light vehicles (category 1) and medium vehicles (category 2) was set to the registered speed limit (30 km/h or 40 km/h) of the corresponding road segment (as defined by the Swedish National Road database – *NVDB*) and was the same for all time periods (daytime 06:00–18:00, evening 18:00–22:00, night-time 22:00–06:00). The distribution of the traffic per vehicle category (light, medium) for different time periods of the day (day, evening, and night) follows Malmö municipality's rule of thumb for light vehicles and the recommended composition for residential roads as stated in Kragh *et al.* [39] for medium vehicles (Table 1). The recommended traffic distribution of light vehicles on residential roads stated in Kragh *et al.* [39] (day: 0.80, evening: 0.10, night: 0.10) is not much different from Malmö municipality's rule of thumb, but the latter was preferred since it is based on years of experience measuring traffic in the area. No such information was available for heavy vehicles.

Information on traffic intensity (total number of vehicles) per vehicle category and time of day was estimated based on the following equations:

$$LV_{\text{day}} = 0.76 \times \left(\left(100 - \frac{HV_{2020}}{100} \right) \times MVD_{2020} \right), \quad (1)$$

$$LV_{\text{evening}} = 0.17 \times \left(\left(100 - \frac{HV_{2020}}{100} \right) \times MVD_{2020} \right), \quad (2)$$

$$LV_{\text{night}} = 0.07 \times \left(\left(100 - \frac{HV_{2020}}{100} \right) \times MVD_{2020} \right), \quad (3)$$

$$MV_{\text{day}} = 0.85 \times \left(\left(\frac{HV_{2020}}{100} \right) \times MVD_{2020} \right), \quad (4)$$

$$MV_{\text{evening}} = 0.05 \times \left(\left(\frac{HV_{2020}}{100} \right) \times MVD_{2020} \right), \quad (5)$$

$$MV_{\text{night}} = 0.10 \times \left(\left(\frac{HV_{2020}}{100} \right) \times MVD_{2020} \right), \quad (6)$$

Table 1: Traffic composition per vehicle category and time of day

Vehicle category	Traffic composition for Day (06:00–18:00)	Traffic composition for Evening (18:00–22:00)	Traffic composition for Night (22:00–06:00)	Source
Light vehicles (category 1)	0.76	0.17	0.07	Malmö municipality
Medium vehicles (category 2)	0.85	0.05	0.10	Table 5 in Kragh <i>et al.</i> [39]



Figure 3: The five LODs of CityGML 2.0 From “An improved LOD specification for 3D building models,” by Biljecki et al. [73].

where LV_{day} , LV_{evening} , and LV_{night} correspond to the total number of light vehicles per a certain time period of a day (daytime, evening, and night), while MV_{day} , MV_{evening} , and MV_{night} refer to the corresponding values for medium vehicles. HV_{2020} represents the percentage of traffic consisting of medium heavy vehicles and MVD_{2020} represents the total number of vehicles per weekday for 2020.

Noise simulation software requires information on noise-obstructing objects (buildings, noise barriers, etc.). In our study, we only consider 3D buildings available as CityGML LOD2 geometries (Figure 3) retrieved from Malmö municipality’s 3CIM data. As most noise simulation software can only handle CityGML LOD1 buildings [66,71,72], the dataset was transformed to CityGML LOD1 with the height of every building set to the highest point of its equivalent CityGML LOD2 version.

Since noise simulations are computationally demanding and time-consuming, an effort was made to limit the number of receivers and simulations without compromising the quality of the analysis. For this purpose, noise simulations were executed for receivers placed at 1.5 m above ground and at 0.1 m from the building façade with a horizontal distribution in accordance with the CNOSSOS-EU model [74].

2.4 Noise simulations

A total of 1,468 receivers were placed on the façades of 22 buildings in our study area. We divided buildings with receivers into five groups and executed noise simulations over the entire study area for each one of those groups for different LC input datasets. Every simulation took 2–7 days to execute depending on the total number of receivers as well as on the total number of LC objects included in the LC dataset (PKO and AIO having the larger amount of LC objects) of that run. The computer used had a 64 GB RAM and a 12-Core processor with 3.5 GHz clock speed.

The noise simulations were executed in SoundPLAN v.9.0 [75] implementing the Nord2000 NPM for the estimation of external noise (L_{den} SE road with dB-weighting = dB

(A)) from car traffic exclusively. Because 3D receiver points were imported manually, a single-point noise simulation was executed instead of a façade noise simulation. SoundPLAN’s standard meteorology data for Sweden were used (i.e. weather statistics: 13 cl. for Sweden). The type of asphalt for the urban roads was set to SMA 11, since it is the most common type of asphalt in Sweden [76]. The building reflectance coefficient was set to 0.8 (recommended default value stated in [66]) while the option to create ground effect areas from road surfaces was enabled. The number of reflections was set to 3 (i.e. reflection order = 3). The maximum search radius from the source was 500 m, the maximum reflection distance from the receiver was 200 m, and the maximum reflection distance from the source was 50 m. Even so, data included in the simulation were limited to the extent of the study area. The allowed tolerance was 0.1 dB and held for each source contribution level.

According to END [20], L_{den} and L_{night} are mandatory indicators for strategic noise mapping, these measures were therefore used to conduct the simulations. L_{den} is the primary noise metric, which indicates annoyance from continuous exposure to noise with additional weighting values being attached to the levels occurring during the evening (5 dB) and night (10 dB) periods (Equation (7)).

$$L_{\text{den}} = 10 \cdot \log \frac{1}{24} \left\{ T_{\text{day}} \cdot 10^{\frac{L_{\text{day}}}{10}} + T_{\text{evening}} \cdot 10^{\frac{L_{\text{evening}}+5}{10}} + T_{\text{night}} \cdot 10^{\frac{L_{\text{night}}+10}{10}} \right\}, \quad (7)$$

where T_{day} , T_{evening} , and T_{night} denote the number of hours within each period (day, evening, and night) periods. L_{day} , L_{evening} , and L_{night} represent the A-weighted long-term average noise levels for these time periods. The time periods for Sweden are the following:

- day: 06:00–18:00 ($T_{\text{day}} = 12$ h),
- evening: 18:00–22:00 ($T_{\text{evening}} = 4$ h),
- night: 22:00–06:00 ($T_{\text{night}} = 8$ h).

Here, L_{night} represent the A-weighted long-term average noise levels during the night (22:00–06:00).

2.5 Statistical comparison methods

Several processing steps were taken to enable the statistical comparison of the LC datasets. The LC classes of every LC dataset were grouped to a common NS-LC level (NS-LC L2) to be comparable. For instance, all vegetation-related NS-LC classes (e.g. *grass*, *bush*, and *forest*) have been grouped to *low vegetation* (NS-LC L2) in the NMDa plot. Similarly, all hard surfaces (asphalt, concrete, gravel, cobblestone, etc.) have been grouped to their superclass *other built-up areas* (NS-LC L2) in the NMDm and PKO LC datasets. Additionally, to track what LC changes have occurred when switching LC layers, all LC datasets were rasterized following the same spatial resolution as the orthophoto (0.08 m). Then, each NS-LC L2 class received a unique integer value for every LC dataset. By subtracting the LC integer values between two LC datasets, it was possible to determine if a raster cell had maintained or changed its LC classification. The results are presented in maps, donut charts, and histograms.

The following processes take place to determine how much the different LC datasets influence the simulated noise levels. General statistics (e.g. min, max, mean, median, and standard deviation) are computed over the differences between pairs of noise simulation outputs produced with different LC input datasets. The results are presented in tabular format. Then, relative cumulative frequency graphs and histogram plots are produced to investigate potential patterns of deviating results. A two-tailed, two-sample equal variance *t*-test is used to determine the significance of the spotted differences. Finally, to get a sense of how changes in LC affect simulated sound levels, illustrations presenting a combination of the location of receivers with the highest detected dB(A) differences and background maps depicting the difference in flow resistivity between LC datasets are produced.

3 Results

Section 3.1 presents the result of the comparison of the LC datasets while Section 3.2 presents the results of the noise simulations.

3.1 Comparison of LC data

The donut plots show the percentage of the study area classified as *low vegetation*, *building surface*, *road and railway surface*, *water*, or *other built-up surfaces* in accordance with NS-LC L2 for the four LC datasets (Figure 4). The largest percentage of vegetation-classified area is observed

in NMDa (61.1%), with NMDm (45%) and PKO (44.3%) showcasing similar percentages, and AIO having the smallest percentage (40.6%). Areas classified as building are relatively similar in all LC datasets, except for a slight overrepresentation in NMDm and a corresponding underrepresentation in NMDa. *Road surfaces* are overrepresented in both NMDa and NMDm compared to PKO and AIO. The percentage of areas classified as *other built-up surfaces* varies substantially between the datasets. *Water* is only included in the NMDa and PKO datasets covering the same percentage of the study area.

Figure 4 depicts the maps presenting LC information for all four LC datasets according to NS-LC L2. The AIO and PKO maps are the ones that look most alike and resemble the orthophoto, while the NMDa and NMDm maps (having a 10-m spatial resolution) look pixelated and fail to accurately represent hard surfaces that do not correspond to buildings or main roads (e.g. pavements, paved inner yards, walking paths, bicycle lanes, etc.). In comparison to the other maps, vegetation is clearly overrepresented in the NMDa map.

Figure 5 displays the LC differences observed when comparing one LC dataset to another. The columns present changes in LC per NS-LC L2 class as percentage bar plots for all LC changes occurring when comparing a specific pair of LC datasets (the sum of every column is 100%).

From Figure 5 it becomes evident that the most similar LC datasets are PKO and AIO with 87.07% of their areas having been classified with the same LC class. The least similar datasets are the NMDa and AIO (58.27% commonly classified areas), and NMDa and PKO (60.86% commonly classified areas). NMDa and NMDm are 79.23% similar. Overall, the largest LC changes occur in the *vegetation* class particularly when converting areas of this class to *other built-up areas*. A smaller percentage of areas are also experiencing LC changes transforming *building surfaces* to *vegetation* or *other built-up areas*. A similar pattern is observed for *road surfaces* being converted to *vegetation* or *other built-up areas*. A small percentage of *other built-up areas* are converted to *vegetation*, *road surfaces*, and *building surfaces*. The smallest area percentage LC changes are observed for the *water* LC class.

3.2 Comparison of noise simulation output

Table 2 shows the min, max, median, mean, and standard deviation of the noise simulation output (L_{den} , L_{day} , and L_{night}) difference between pairs of LC datasets. The difference is expressed in dB(A).

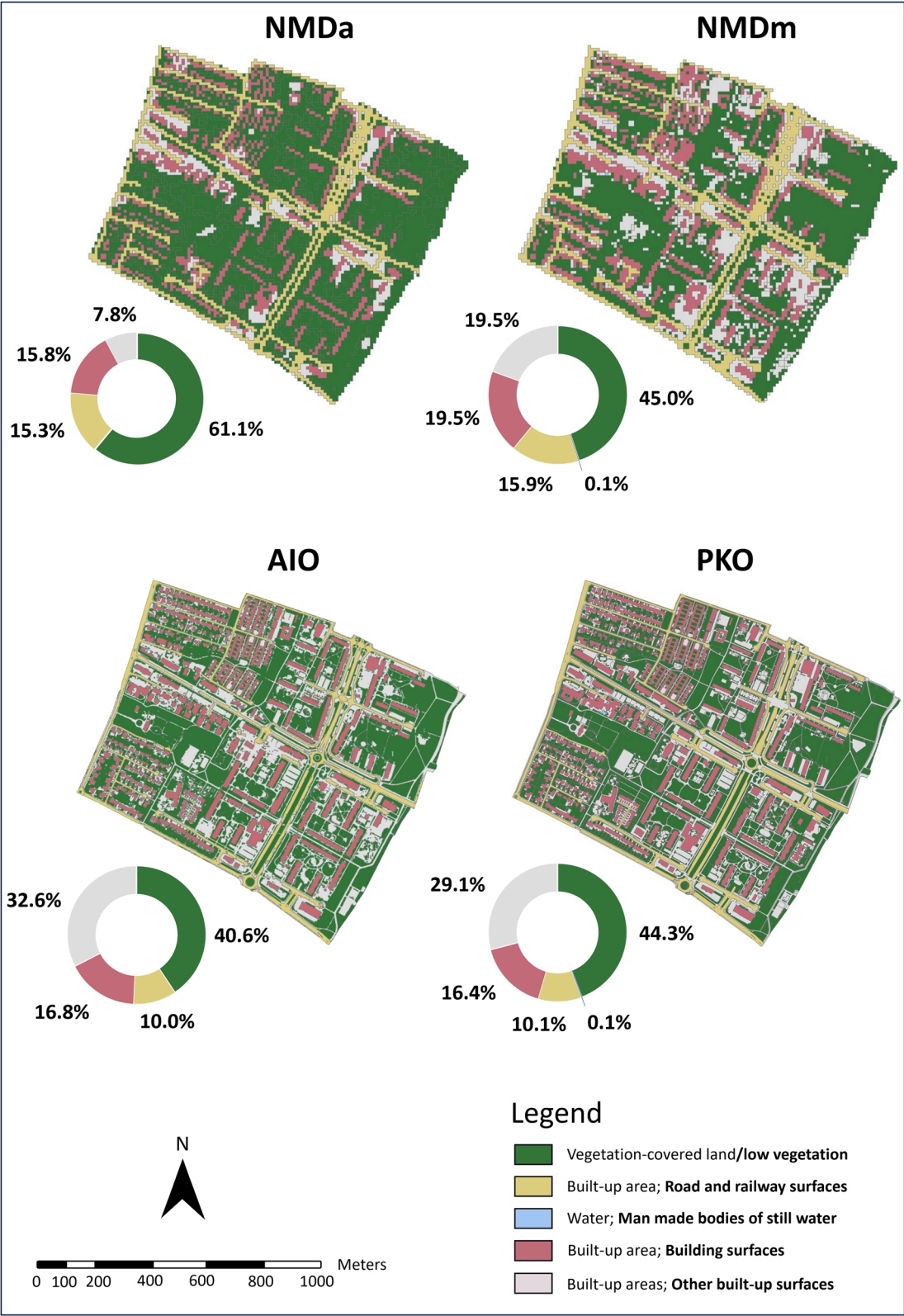


Figure 4: Donut plot presenting the percentage of the study area covered by every NS-LC L2 thematic class. The maps provide a descriptive illustration of the study area's LC classification results per dataset.

LC changes	NMDa to NMDm (conversion)	NMDa to PKO (conversion)	NMDm to PKO (conversion)	NMDa to AIO (conversion)	NMDm to AIO (conversion)	PKO to AIO (conversion)
Unchanged	79.23 %	60.86 %	66.49 %	58.27 %	65.37 %	87.07 %
From Vegetation						
to Buildings	3.24%	4.51%	2.11%	4.90%	2.40%	0.88%
Roads	0.79%	1.24%	0.48%	1.21%	0.47%	0.02%
Other built-up areas	13.37%	17.89%	9.37%	20.18%	10.90%	5.47%
Water	0.02%	0.05%	0.04%	0.00%	0.00%	0.00%
From Buildings						
to Vegetation	0.40%	2.75%	3.49%	2.11%	2.61%	0.18%
Roads	0.04%	0.04%	0.03%	0.03%	0.02%	0.001%
Other built-up areas	0.29%	2.33%	3.20%	3.10%	4.17%	1.29%
Water	0.01%	0.01%	0.01%	0.00%	0.00%	0.00%
From Roads						
to Vegetation	0.34%	2.32%	2.25%	2.20%	2.16%	0.01%
Buildings	0.10%	0.26%	0.19%	0.29%	0.23%	0.00%
Other built-up areas	0.12%	4.35%	4.59%	4.54%	4.72%	0.85%
Water	0.00%	0.003%	0.0001%	0.00%	0.00%	0.00%
From Other built-up areas						
to Vegetation	0.67%	1.90%	5.52%	1.56%	4.56%	2.50%
Buildings	1.06%	0.92%	1.32%	0.99%	1.43%	0.96%
Roads	0.31%	0.55%	0.86%	0.60%	0.88%	0.77%
Water	0.03%	0.02%	0.02%	0.00%	0.00%	0.00%
From Water						
to Vegetation	0.00%	0.00%	0.01%	0.00%	0.01%	0.01%
Buildings	0.00%	0.00%	0.004%	0.00%	0.01%	0.01%
Roads	0.00%	0.00%	0.00%	0.00%	0.00%	0.00%
Other built-up areas	0.00%	0.00%	0.03%	0.00%	0.04%	0.07%

Figure 5: Percentage area of the study area that has retained or changed its LC classification when comparing two LC datasets. Columns correspond to LC changes occurring when comparing two LC datasets (the total sum of percentage areas in a column is 100%). Rows show the results per NS-LC L2 class for all LC dataset pair comparisons.

In general, noise simulation output produced using different LC datasets as input differs from -2.7 to $+3.3$ dB(A) (Table 2). The largest noise simulation output differences are spotted for L_{day} (0 – 3.3 dB(A)) while the

differences are somewhat smaller for L_{den} (0 – 3.0 dB(A)) and smallest for L_{night} (0 – 2.6 dB(A)). The LC dataset generating the greatest differences in noise simulation output compared to the others is NMDa. In this case, the average

Table 2: Statistical results of difference in simulation noise output produced by the four LC datasets

LC datasets (difference)	L_{den} (dB(A))					L_{day} (dB(A))					L_{night} (dB(A))				
	Min	Max	Median	Mean	Std	Min	Max	Median	Mean	Std	Min	Max	Median	Mean	Std
NMDm-NMDa	-0.1	3.0	0.6	0.8	0.5	-0.1	3.3	0.7	0.9	0.6	-0.1	2.6	0.6	0.7	0.5
PKO-NMDa	-0.8	2.2	0.6	0.6	0.4	-0.8	2.3	0.6	0.7	0.5	-0.8	2.1	0.5	0.5	0.4
PKO-NMDm	-1.8	1.5	-0.1	-0.2	0.5	-2.1	1.5	-0.1	-0.2	0.6	-1.5	1.3	0.0	-0.1	0.5
AIO-PKO	-0.9	1.3	-0.1	0.0	0.3	-0.9	1.5	-0.1	-0.1	0.3	-0.7	1.3	0.0	0.0	0.2
AIO-NMDa	-1.0	2.5	0.5	0.6	0.5	-1.1	2.9	0.6	0.6	0.5	-0.8	2.1	0.5	0.6	0.4
AIO-NMDm	-2.4	1.6	-0.2	-0.2	0.5	-2.7	1.8	-0.2	-0.3	0.5	-2.0	1.3	-0.1	-0.1	0.4

difference lies between 0.5 and 0.9 dB(A), which with the addition of the standard deviation, amounts to a difference ranging from 0.1 to 1.5 dB(A).

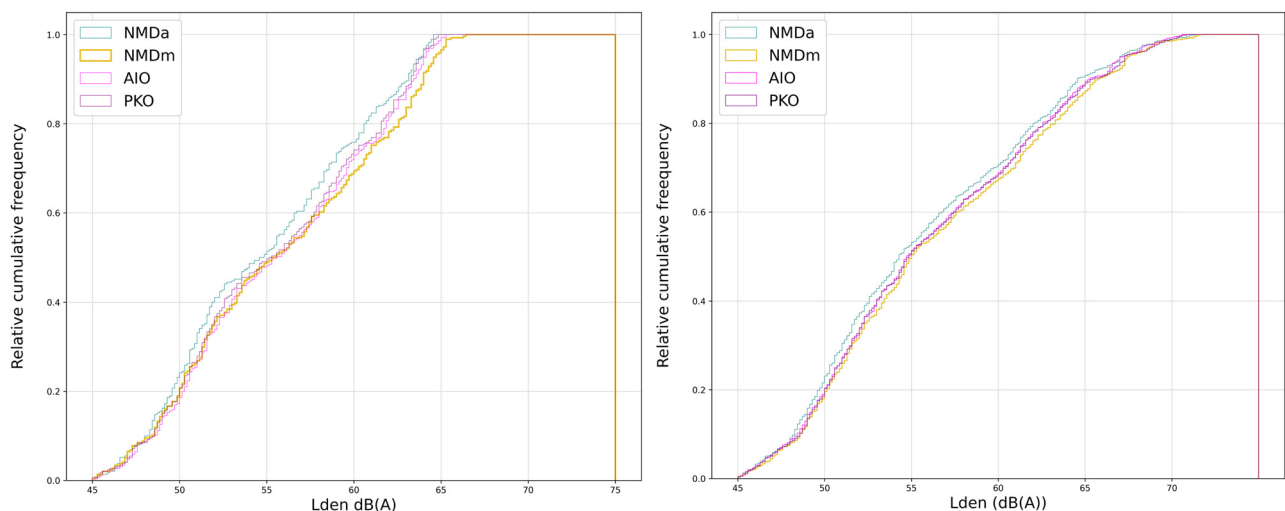
Figure 6 presents two relative cumulative frequency plots of the total number of receivers having a certain L_{den} dB(A) value for simulations executed using each one of the LC datasets. The left plot includes simulation output from receivers placed on buildings in a subpart of the study area (BS6 in Figure 1), while the right plot presents results from all the receivers in the study area. Figures 7 and 8 present the same information as Figure 6 but for L_{day} and L_{night} correspondingly.

Simulated noise levels for all LC datasets seem to follow similar patterns when looking at the L_{den} , L_{day} , and L_{night} relative cumulative frequency graphs for all receivers in the study area (the right plot in Figures 6–8). The only exceptions being NMDa showcasing more receivers with lower dB(A) values and NMDm showcasing more receivers with slightly higher dB(A) values. This pattern

becomes more prominent when focusing on subparts of the study area (left plot in Figures 6–8).

The histogram in Figure 9 shows the distribution of L_{den} noise levels produced by noise simulations using different LC input datasets. The noise simulation distribution can be approximated with a normal distribution with means and standard deviations that are almost identical for the outputs produced using the AIO, and PKO LC datasets as input. The distribution curve for noise simulation output generated using NMDa as input deviates from the others, indicating more receivers with lower dB(A) values, while the corresponding distribution curve for NMDm indicates the existence of more receivers with higher dB(A) values.

To investigate whether the spotted differences are significant, we implemented a t -test where the null hypothesis was that L_{den} , L_{day} , and L_{night} noise levels do not differ significantly between noise simulation outputs generated using different LC datasets. The results of the t -test (t -value and

**Figure 6:** Relative cumulative frequency graph of noise simulation output in L_{den} (left: receivers placed on buildings in BS6, right: all receivers in the study area) for the four different LC datasets.

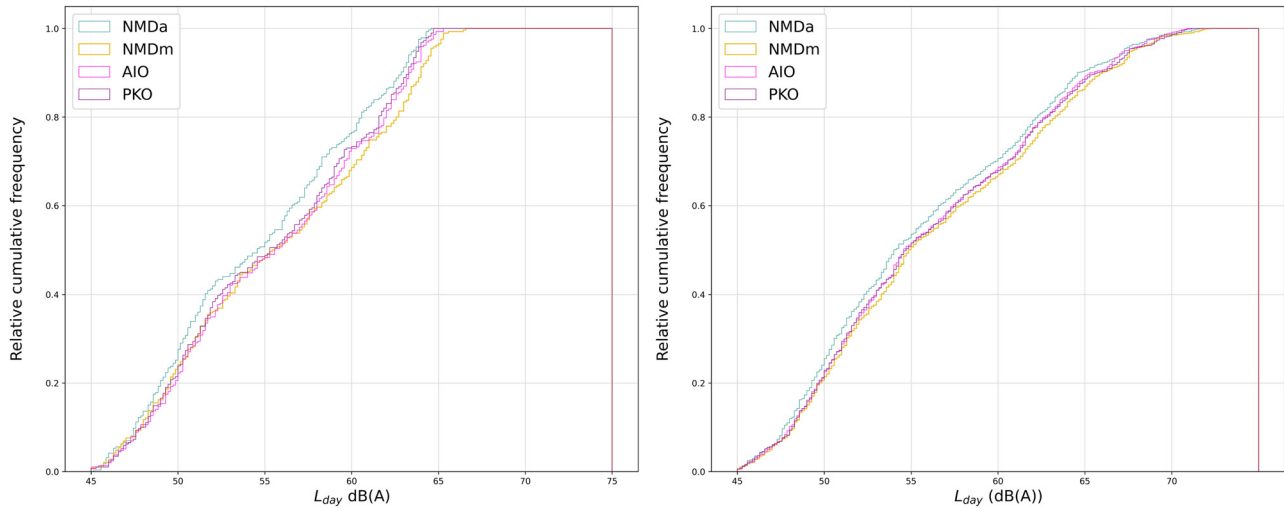


Figure 7: Relative cumulative frequency graph of noise simulation output in L_{day} (left: receivers placed on buildings in BS6, right: all receivers in the study area) for the four different LC datasets.

p -value) performed on pairs of noise simulation outputs are presented in Table 3.

The difference in noise levels produced by simulations using different LC datasets as input is statistically significant for all L_{den} , L_{day} , and L_{night} noise levels when comparing NMDa to the other LC datasets (see rows with values in bold format in Table 3).

The largest mean difference in dB(A) values between noise simulations was observed for L_{den} between NMDa and the other LC datasets. To analyse this, Figure 10 was created to explore the spatial distribution of LC changes (shown as difference in *flow resistivity*) in relation to L_{den} dB(A) noise-level differences. Every LC geometry was assigned

with an LC class and corresponding flow resistivity value (Table A4). The background maps (Figure 10) depict differences in flow resistivity between NMDa and the other LC datasets as well as a selection of receivers whose L_{den} (dB(A)) difference was equal or greater than 2 dB(A) when comparing NMDa simulation output to simulation output generated using other LC datasets. It should be mentioned that all highlighted receivers have an L_{den} value greater or equal to 53 dB(A). When comparing PKO with NMDa noise levels, 11/1,468 receivers (0.8%) showcase a L_{den} diff >2 dB(A) while having a $L_{den} > 53$ dB(A). When comparing AIO with NMDa noise levels, 17/1,468 receivers (1.2%) meet those requirements and, finally, when comparing NMDm to NMDa noise levels, 71/

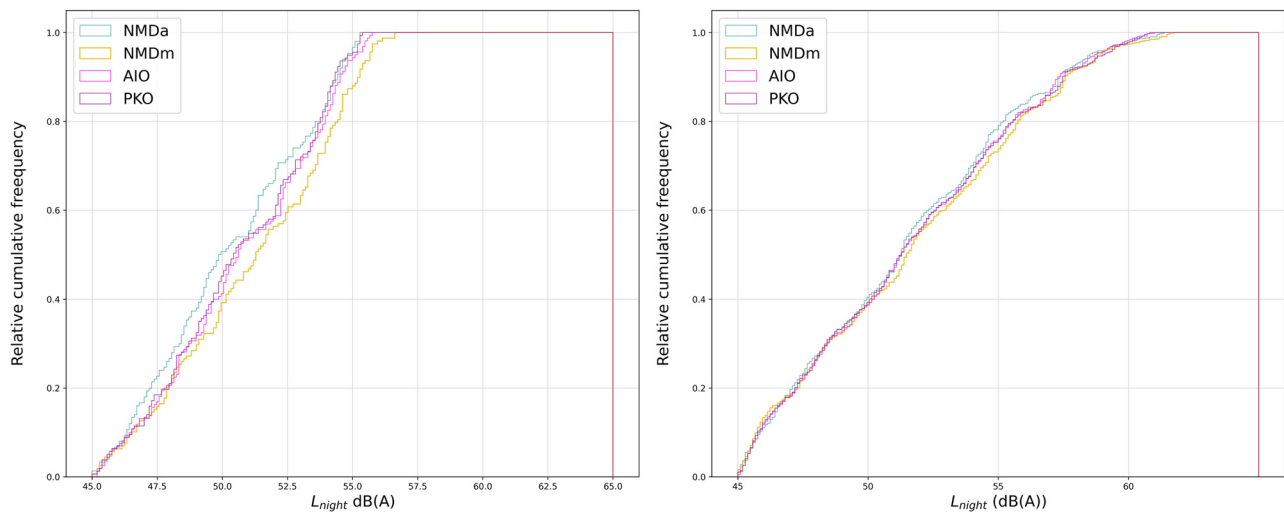


Figure 8: Relative cumulative frequency graph of noise simulation output in L_{night} (left: receivers placed on buildings in BS6, right: all receivers in the study area) for the four different LC datasets.

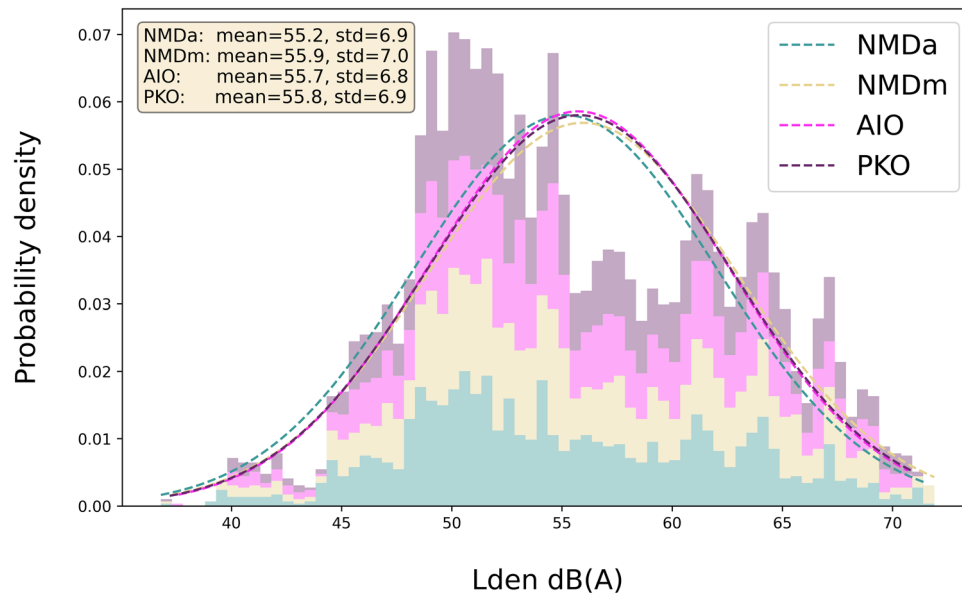


Figure 9: Histograms and distributions of simulated L_{den} noise levels produced using the four LC input datasets.

1,468 receivers (4.8%) do the same. The largest differences in L_{den} noise levels are observed for receivers being placed on buildings close to the most trafficked roads (Figures 2 and 10). Examining the background maps in Figure 10, it is becoming obvious that the other LC datasets have more surfaces with higher flow resistivity values (purple-shaded areas) compared to NMDa.

During the manual digitization of the LC datasets NMDm and PKO, several LC types that were not included in the NS-LC emerged. Typical examples are surfaces covered by wood (e.g. patios, staircases), glass (greenhouses), grass concrete (grass concrete paver), metal (temporary platforms, metal roofs), and grass (green roofs) (Figure 11). In PKO wooden surfaces cover 0.25% (2,342 m²), grass concrete pavers 0.16% (1,551 m²), and glass roofs 0.009% (80 m²) of the study area. In NMDm green roofs cover 0.07% (700 m²) of the study area.

4 Discussion

According to our LC comparison, NMDa overestimates vegetation-covered areas. This is likely because NMD was initially produced to facilitate environmental monitoring and therefore applied rules that prioritized *vegetation* (cf. 2.2.1). Another factor contributing to the overrepresentation of *vegetation* in NMDa is that the satellite imagery does not capture the ground surface beneath vegetation. Besides tall trees with dense foliage covering hard surfaces like asphalt roads (Figure A1), there are cases where vegetation on balconies of tall buildings and green roofs have been classified as *forest* (Figures A2 and A3), vegetation on building facades having been classified as *forest* or *vegetation* (Figure A4) and climbing plants growing on external walls being classified as *vegetation* (Figure A5).

It is worth mentioning that, at its current state, NS-LC does not allow distinguishing buildings with different types

Table 3: T-test results examining the significance of the difference between simulated L_{den} , L_{day} , and L_{night} noise levels produced by a pair of different LC datasets. Bold values rows correspond to statistically significant noise level dB(A) differences

Comparisons	L_{den}			L_{day}			L_{night}		
	Mean difference (dB(A))	t-Value	p-Value	Mean difference (dB(A))	t-Value	p-Value	Mean difference (dB(A))	t-Value	p-Value
NMDm-NMDa	0.8	3.07	0.002	0.9	3.32	0.001	0.7	2.75	0.006
PKO-NMDa	0.6	2.44	0.015	0.7	2.61	0.009	0.5	2.23	0.026
PKO-NMDm	-0.2	0.65	0.518	-0.2	0.74	0.462	-0.1	0.54	0.589
AIO-PKO	0.0	0.16	0.874	-0.1	0.25	0.804	0.0	0.03	0.974
AIO-NMDa	0.6	2.30	0.022	0.6	2.38	0.018	0.6	2.21	0.027
AIO-NMDm	-0.2	0.81	0.420	-0.3	0.99	0.325	-0.1	0.58	0.565

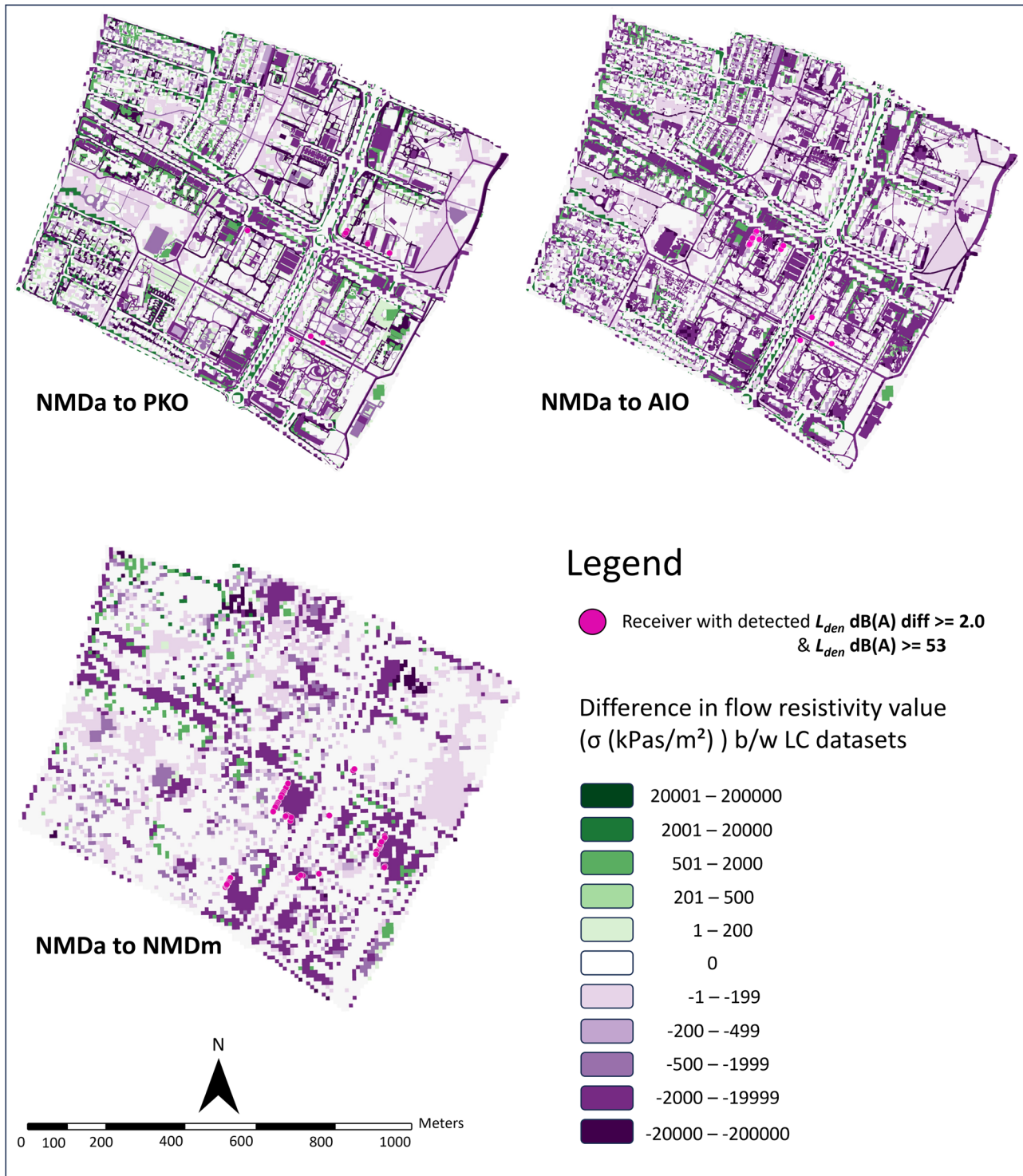


Figure 10: Maps presenting noise simulation output based on the 24 h L_{den} metric, highlighting receivers with $L_{den} \geq 53$ dB(A) in both LC datasets, and whose corresponding difference is at least 2 dB(A). A background map depicting changes in flow resistivity values when subtracting NMDa flow resistivity values from the flow resistivity values of another LC dataset is used to show the spatial relevance between changes in flow resistivity and changes in simulated L_{den} noise levels.



Figure 11: Examples of wooden surfaces (left), grass concrete pavers (middle-left), and green roofs (middle right and right) found in urban settings.

of roofs (clay tiles, green roof, solar tiles, metal roofing, wood roofing, asphalt shingle, *etc.*). Adding roof material to the NS-LC classification at L4 (A. Persson, Lund University, Department of Physical Geography and Ecosystem Science, Lund, personal communication, September 17, 2024) could be significant from a noise propagation perspective since green roofs have totally different flow resistivity values compared to other roof materials [77].

Vegetation is a bit underrepresented in AIO compared to the other LC datasets, but this could be attributed to some vegetated surfaces (*e.g.* grass lawns) being shaded by tall trees, bushes or buildings and the AI classification algorithm classifying those pixels as *other built-up areas* instead (Figures 4 and 5). Kuras *et al.* [78] have implemented a technique incorporating LiDAR with hyperspectral data to eliminate the effect of shadows based on the difference in height that is detectable with LiDAR data.

Ground surface areas classified as *buildings* are almost identical in AIO and PKO with the 0.4% difference possibly being attributed to the resolution of the orthophoto used in the AI LC-classification method. NMDa and PKO have similar percentages of building-covered surfaces, despite the fact of the Swedish Environmental Protection Agency implementing the algorithm that only classifies a cell as “building” if its centroid is covered by a building footprint. The NMDm shows a greater number of areas covered by buildings compared to the rest of the LC datasets. This is caused by implementing the majority rule on raster cells of coarse resolution (10 m).

Road areas are greatly overestimated in both NMD datasets due to their coarse spatial resolution. An additional reason in the NMDa LC dataset’s case, is the implementation of the priority rule ensuring that main roads are represented by adjacent raster cells. AIO and PKO produce the same percentages of areas classified as *road*.

Areas classified as *other built-up areas* are underrepresented in both NMD datasets, more so in NMDa as it favours *vegetation* over this LC class. However, this class is overrepresented in AIO mainly because shaded areas or areas not been deemed suitable for any other LC class, were classified as *other built-up areas*.

Areas covered by *water* are only present in NMDm and PKO. AIO does not include any areas classified as *water* due to a lack of training data for water-covered urban areas (*e.g.* swimming pools, ponds). NMDa does only classify a surface as *water* if it is larger than 100 m², which affects its representation of swimming pools, canals, and ponds in cities.

From Figures 4 and 5, it is evident that PKO and AIO have the highest level of resemblance with almost 90% of their areas being covered by the same hard or soft surface followed by NMDa and NMDm with 79.23% of resemblance, while NMDa and AIO are the most different with only 58.27% of their common area maintaining its initial surface classification. When comparing AIO’s and PKO’s differences from NMDa, the surfaces whose LC classification has changed from hard to soft or the contrary are scattered evenly over the study area (Figure 10). This indicates that the differences are occurring randomly and could therefore be a consequence of the coarser spatial resolution (10 m) of NMDa. The surfaces changing LC classification in the PKO and AIO difference map (Figure 10) are predominantly doing so from soft to hard and are relatively scattered. When looking at the maps depicting the difference between PKO, AIO, and NMDm from NMDa, the areas maintaining their original LC classification are fewer while those that change LC include both larger areas at certain locations as well as smaller areas scattered all over the study area. Changes in LC classification in this case could be attributed to both the coarser spatial resolution of NMDa

(smaller areas changing LC classification) but also to NMD's priority rules (larger areas changing LC classification). Another possible reason for changes covering larger areas when comparing PKO to the other LC datasets and the main reason behind differences between PKO and AIO is the fact that the municipality basemap used for producing it is more recent than the orthophoto with some areas having been densified (green areas turned into buildings or parking lots). This is an example where the updating frequency of remotely sensed imagery is too low, and raising this frequency becomes increasingly important in urban areas undergoing rapid development.

Though the quality and spatial resolution of LC has been proven to have a significant influence on noise propagation from airborne traffic in urban areas [79], this is not as prominent when studying noise propagation from car traffic in our study area. Noticeable differences are spotted on a local scale (BS6), but these differences are somewhat smoothed out when switching the focus to the entire study area (Figures 6–8). Generally, simulated outputs differ by about ± 3 dB(A), as shown in Table 2. The largest differences in dB(A) values are observed for simulated noise values during daytime (L_{day}) when comparing the NMDa to the NMDm, PKO and AIO LC datasets (Table 2). Differences between L_{den} , L_{day} , and L_{night} simulation output produced by using NMDa compared to simulation output produced using the other LC datasets are on average close to 1 dB(A) with a max difference of 3.0 dB(A) L_{den} and statistically significant (Table 3), indicating that NMDa is not the best choice of LC dataset for noise analyses in urban settings. This becomes even more important when considering that the largest differences occur on locations close to noise sources (most trafficked roads) where NMDa surfaces have changed from hard to soft and the observed noise level is greater or equal to the WHO recommended threshold of 53 dB(A) L_{den} (Figure 10).

Sound travels faster during daytime due to high air temperature with humidity increasing that speed even further. Additionally, during daytime sound waves bend away from the ground, but typically, during night-time, because of more stable atmospheric conditions (or even temperature inversion), sound waves bend towards the ground. Consequently, at night, distant sounds can be heard as the sound waves get refracted and reach receivers from distant sources. In cities like Malmö, where humid or windy cold nights are not unusual for a great part of the year (air temperature varies from -12 to 29°C [80] while the annual average relative humidity is 81% [81] and wind speed varies from 0.0 to 13 m/s with the wind predominantly blowing from SW and NW directions [82]), living in ground floor apartments of buildings close to larger urban roads may significantly disturb sleep quality. This is due to the combined effect of the noise source being so

close (road), ground surfaces close to the receivers being hard (e.g. pavement) and because of stable atmospheric conditions (which typically occur at night) making sound waves from car traffic pointing downwards hitting those hard surfaces close to the windows (located at 1.5 m above ground, i.e. same as receiver height). The same goes for the early morning hours that are cold and humid and would lead to higher noise levels disturbing people in schools, day-cares, and offices located on the ground floor of buildings close to busy roads. In both cases, using the NMDa LC dataset (a dataset that overrepresents vegetation and underrepresents hard surfaces) in the noise simulation would underestimate the noise at the building façade with true L_{den} values exceeding the WHO recommended threshold of 53 dB(A) for the highlighted receivers (Figure 10).

NMDa is the LC dataset requiring the least amount of pre-processing by the user before importing it to noise simulation software, but since it yields significantly different noise level estimations for both daytime and night-time, when maintaining low noise levels is so important for health and productivity, it could be worth looking at other alternatives. Noise simulations utilizing NMDm produce somewhat higher noise levels compared to AIO and PKO. However, those outputs are still quite similar, indicating that the priority rules applied in the LC classification algorithm can be more influential than the spatial resolution. This observation is especially important considering our study area is characterized by a mixed LC. Therefore, a spatial resolution of 10 m could potentially be enough for representing LC in urban areas depending on the choice of priority rules. However, considering the difference in simulated noise between NMDm and PKO or AIO, it is doubtful whether a coarser resolution would be good enough. Consequently, the suitability of other open-access LC datasets such as CORINE having an even coarser resolution is not favourable. Additionally, NMD, Urban Atlas, and CORINE have very low temporal updating frequencies, with Urban Atlas only providing LC information for a subset of urban areas in Europe.

AI-generated LC layers are a promising alternative for rapid LC dataset production, under the condition that aerial and satellite imagery are accessible and updated frequently, adequate training dataset are openly available, and AI-algorithms and workflows are easy to access or implement. Manually digitized LC datasets may be more representative but are time-consuming and expensive to produce. Regardless of what LC data is chosen, storing it in a semantic 3D city model may assist in sharing the updating tasks among municipality divisions and avoid overlaps and redundancy, ultimately contributing to an up-to-date and accessible LC layer for all actors involved in the urban planning process.

NS-LC should include thematic classes corresponding to all materials (including wood and concrete grass pavers) often found in urban settings. For NS-LC to be suitable for noise simulations, it is important that when aggregating NS-LC levels of detail then the flow resistivity value associated with the aggregated LC class is representative for all the LC classes included in the higher NS-LC levels.

Currently, this is achieved for most of the themes, the only exceptions being the *buildings* (e.g. depending on the material used on the building's exterior or roof, this can affect the flow resistivity) and *other built-up areas* where *excavated ground* NS-LC L4 is supposed to have the same flow resistivity value as *concrete* NS-LC L4 when aggregated to *built-up areas* in NS-LC L1-L3. Additionally, as stated by Gustafson and Genell [61], new noise measurements are required to determine the flow resistivity of all urban surfaces included in the NS-LC. As flow resistivity values are greatly influenced by climate [83], it might be advisable for countries with non-uniform climates to include multiple flow resistivity tables depending on what climate zone each of their regions belongs to.

We have chosen to execute the noise simulations using SoundPLAN v.9.0 as it is considered one of the most used noise simulation software [84,85] and because it has implemented NPMs such as Nord2000 [84]. We did not try to execute the same simulations in any other noise simulation software.

The results found in this study correspond to a local or street scale area characterized by a mixed LC composition in a climate typical for a coastal city in southern Sweden. It would be interesting to repeat the experiments for more and larger areas with varying LC compositions under similar climate conditions. Our study area, though it includes many LC classes, is quite flat. Examining the influence of LC on locations with more varying topography would be interesting. Also, investigating the influence of LC on urban areas of different climates would be advisable [83].

Only simulation results for receivers placed at 1.5 m above ground were included in the study. Noise simulations for receivers placed at 4.0 m above ground were also performed, but only for a smaller area (see BS1 in Figure 1). The produced results were similar for all LC datasets. Examining if and to what extent different LC datasets influence the noise detected at receivers placed on different horizontal levels (heights) of building facades was not part of this study. This would however be interesting to study in more densely built-up areas with taller buildings or in areas with varying topography.

We used a small search radius (500 m), even though 1–1.5 km is the usual recommended search radius when conducting environmental noise simulations [37]. This was done

to limit the execution time. Additionally, as the extent of our study area was approximately 1,000,000 km² and because most of our receivers were placed on buildings close to its centre, this meant that we got the influence of noise sources (road traffic) from the entire study area for most receivers. However, it should be noted that the purpose of this study was not to provide the most accurate noise simulation output, but rather to detect changes in noise simulation output caused by using different LC datasets as input.

5 Conclusion

In this study, we have examined the effect of using different land cover (LC) datasets as input to noise simulations. The largest effect, resulting in up to 3.3 dB(A) difference in simulated L_{day} values, stems from a combination of priority rules implemented when producing the LC datasets and what data were used to produce the LC datasets. The satellite-based (Sentinel-2; 10 m spatial resolution) NMDa LC dataset whose production rules prioritize vegetation, could not adequately identify LC under canopies. This dataset contained a substantially larger proportion of vegetation compared to the study's other three LC datasets, resulting in significantly lower simulated L_{den} , L_{day} , and L_{night} noise values. From this perspective, it can be considered suboptimal for urban noise analyses. The second satellite-based (Sentinel-2; 10 m spatial resolution) LC dataset, NMDm, that implemented a majority rule to determine the LC class of every raster cell, produced simulated noise levels closer to the AI-generated and manually digitized LC datasets, indicating that priority rules in LC classification are more influential than spatial resolution.

When comparing the output between noise simulations utilizing LC datasets (NMDm) with lower spatial resolution (10 m) to higher spatial resolution (0.08 m) AI-generated LC datasets (AIO) and manually digitized vector LC datasets (PKO), the differences are small (on average less or equal to 1 dB(A)). That is, even though the datasets were produced using different techniques, resulting in non-identical LC representations, they generate similar noise simulation output. However, because of the fine-scale, mixed LC nature of the study area, utilizing LC datasets of lower spatial resolution than 10 m (e.g. CORINE) would not be advisable, since this would fail to represent objects of the urban fabric that substantially influence noise propagation. Nevertheless, a too-fine spatial resolution significantly increases the execution time of noise simulations, in our case leading to a more than doubled execution time. However, this result does not imply that it is acceptable to disregard small 3D barriers (e.g. sound barrier walls) as input to noise simulations; their effect has not been evaluated in this study.

The specifications of LC datasets should ensure that every type of material often found on ground surfaces in urban environments is represented in the corresponding LC classification system. Taking into consideration that most LC datasets are not produced with the objective to represent surfaces of urban environments (e.g. CORINE, NMD), it is natural that some materials (e.g. wood or glass) or structures combining different materials (e.g. grass concrete pavers) are not represented in the classification system. As these materials or structures may have a significant impact on simulations conducted in the urban planning process (including noise as shown in this study), we propose that national agencies take these into account when creating their national specifications for LC. Additionally, if a multiple-level LC representation schema is to be implemented, it is important that higher level LC thematic classes (*concrete, excavated ground, artificial grass, etc.*) have reasonably similar flow resistivity values with their corresponding aggregated (lower level) thematic class (e.g. *other built-up areas*). Finally, to speed up noise analyses, it is paramount to associate every thematic class in the NS-LC with its corresponding flow resistivity based on updated real-world noise measurements inside urban areas.

Moreover, many datasets focus on LU instead of LC, mix the two terms, or are not detailed enough to point to the material of the ground surface (e.g. CORINE, Urban Atlas). Since it is the material of a ground surface and not its use that has different properties (acoustic, spectral, and water absorption), we recommend that LC is prioritized. This is particularly important for the creation of open-access LC datasets that can be used for training AI tools.

Acknowledgements: We would like to thank Malmö municipality for providing the 3D city model used in our study. We would also like to express our gratitude to the Swedish Mapping, Cadastral, and Land Registration Authority (Lantmäteriet) for the constructive discussions and for kindly allowing us to use the current suggestion for NS-LC classifications. We would like to acknowledge the contribution of noise experts Mikael Ögren and Andreas Gustafson for providing their opinions on mapping the NMD LC classes to NS-LC thematic classes and on assigning flow resistivity values for the NS-LC thematic classes. We would like to express our sincere gratitude to the SoundPLAN customer support for engaging in discussions and providing guidance on how to conduct our simulations in the best possible way utilizing the full potential of the software for the purpose of our study. We would like to warmly thank Lovisa Rosenquist Ohlsson for granting us permission to use her exquisite photographs depicting LC examples of the LC classes “marl,” “coniferous shrublands,” and “deciduous shrublands.”

Funding information: This work was supported by the Formas (Swedish Research Council for Sustainable Development) project Facilitating energy and noise simulations in the planning of urban densification [grant numbers 2020-01460]. Support by InfraVis is gratefully acknowledged, Swedish Research Council grant 2021-00181.

Author contributions: All authors have accepted responsibility for the entire content of this manuscript and consented to its submission to the journal, reviewed all the results, and approved the final version of the manuscript. Conceptualization, Karolina Pantazatou; Lars Harrie; Kristoffer Mattisson; methodology, Karolina Pantazatou; formal analysis, Karolina Pantazatou; data creation and data curation, Karolina Pantazatou; Erik Telldén; Anders Kettisen; writing – original draft preparation, Karolina Pantazatou; writing – review and editing, Lars Harrie; Kristoffer Mattisson; Per-Ola Olsson; Erik Telldén; Anders Kettisen; Soraya Hosseinvash Azari; Wenjing Liu; visualization, Karolina Pantazatou; project administration, Lars Harrie; funding acquisition, Lars Harrie.

Conflict of interest: Authors state no conflict of interest.

Data availability statement: The data that support the findings of this study are available from the City of Malmö, but restrictions apply to the availability of these data, which were used under license for the current study, and so are not publicly available. Data are, however, available from the authors upon reasonable request and with permission of the City of Malmö.

References

- [1] United Nations. Population | United Nations. 2022 [cited 2024 Nov 18]; <https://www.un.org/en/global-issues/population>.
- [2] United Nations-Department of Economic and Social Affairs. 68% of the world population projected to live in urban areas by 2050, says UN [Internet]. www.un.org. 2018 [cited 2024 Nov 18]. <https://www.un.org/development/desa/en/news/population/2018-revision-of-world-urbanization-prospects.html>.
- [3] European Environment Agency. urban sprawl [Internet]. 2017 [cited 2024 Nov 18]. <https://www.eea.europa.eu/help/glossary/eea-glossary/urban-sprawl>.
- [4] Pelczynski J, Tomkowicz B. Densification of cities as a method of sustainable development. IOP Conf Ser Earth Environ Sci. 2019;362(1):012106. doi: 10.1088/1755-1315/362/1/012106.
- [5] Tong H, Kang J. Characteristics of noise complaints and the associations with urban morphology: A comparison across densities. Environ Res. 2021;197(111045):111045. doi: 10.1016/j.envres.2021.111045.
- [6] Berghauser Pont M, Forssén J, Haeger-Eugensson M, Gustafson A, Rosholm N. Using urban form to increase the capacity of cities to

- manage noise and air quality. *Urban Morphol.* 2023;27(1):51–69. doi: 10.51347/um27.0003.
- [7] Basner M, McGuire S. WHO environmental noise guidelines for the European region: A systematic review on environmental noise and effects on sleep. *Int J Environ Res Public Health.* 2018;15(3):519. doi: 10.3390/ijerph15030519.
 - [8] van Kempen E, Casas M, Pershagen G, Foraster M. WHO environmental noise guidelines for the European Region: A systematic review on environmental noise and cardiovascular and metabolic effects: A summary. *Int J Environ Res Public Health.* 2018;15(2):379. doi: 10.3390/ijerph15020379.
 - [9] Tobias A, Recio A, Díaz J, Linares C. Does traffic noise influence respiratory mortality? *Eur Respir J.* 2014;44(3):797–9. doi: 10.1183/09031936.00176213.
 - [10] Gupta A, Gupta A, Jain K, Gupta S. Noise pollution and impact on children health. *Indian J Pediatr.* 2018;85(4):300–6. doi: 10.1007/s12098-017-2579-7.
 - [11] Öhrström E. Psycho-social effects of traffic noise exposure. *J Sound Vib.* 1991;151(3):513–7. doi: 10.1016/0022-460x(91)90551-t.
 - [12] Guski R, Schreckenber D, Schuemer R. WHO environmental noise guidelines for the European region: A systematic review on environmental noise and annoyance. *Int J Environ Res Public Health.* 2017 [cited 2024 Nov 18];14(12):1539, <https://www.mdpi.com/1660-4601/14/12/1539>.
 - [13] Clark C, Paunovic K. WHO environmental noise guidelines for the European region: A systematic review on environmental noise and cognition. *Int J Environ Res Public Health.* 2018;15(2):285. doi: 10.3390/ijerph15020285.
 - [14] Weyde KV, Krog NH, Oftedal B, Magnus P, Øverland S, Stansfeld S, et al. Road traffic noise and children's inattention. *Environ Health.* 2017;16(1):127. doi: 10.1186/s12940-017-0337-y.
 - [15] Rosen S, Olin P. Hearing loss and coronary heart disease. *Arch Otolaryngol.* 1965;82:236–43. doi: 10.1001/archotol.1965.00760010238004.
 - [16] European Environment Agency. Environmental Noise in Europe, 2020 [Internet]. [eea.europa.eu. 2020 \[cited 2024 Nov 18\]. https://data.europa.eu/doi/10.2800/686249](https://data.europa.eu/doi/10.2800/686249).
 - [17] Buxton RT, McKenna MF, Mennitt D, Fristrup K, Crooks K, Angeloni L, et al. Noise pollution is pervasive in U.S. protected areas. *Science.* 2017;356(6337):531–3. doi: 10.1126/science.aah4783.
 - [18] European Environment Agency. Health impacts of exposure to noise from transport [Internet]. 2022 [cited 2024 Nov 18]. <https://www.eea.europa.eu/ims/health-impacts-of-exposure-to-1>.
 - [19] World Health Organization. Chapter 11 Environmental noise: Compendium of WHO and other UN guidance on health and environment (WHO/HEP/ECH/EHD/22.01) [Internet]. 2022. Available from: https://cdn.who.int/media/docs/default-source/who-compendium-on-health-and-environment/who-compendium_noise_01042022.pdf.
 - [20] Directive 2002/49/EC of the European Parliament and of the Council of 25 June 2002 relating to the assessment and management of environmental noise - Declaration by the Commission in the Conciliation Committee on the Directive relating to the assessment and management of environmental noise [Internet]. 2002. <http://data.europa.eu/eli/dir/2002/49/oj>.
 - [21] SWS 2010:900. Plan- och bygglag [Planning and Building Act] [Internet]. 2010. https://www.riksdagen.se/sv/dokument-och-lagar/dokument/svensk-forfattningssamling/plan-och-bygglag-2010900_sfs-2010-900/.
 - [22] SFS 2014:902. Lag om ändring i plan- och bygglagen (2010:900) [Act on Amendments to the Planning and Building Act] [Internet]. Lagboken.se. 2014 [cited 2024 Nov 18]. Available from: https://www.lagboken.se/Lagboken/start/fastighetsratt/plan-och-bygglag-2010900//d_2084482-sfs-2014_902-lag-om-andring-i-plan-och-bygglagen-2010_900.
 - [23] SFS 2015:670. Lag om ändring i miljöbalken [Act on Amendments to the Environmental Code] [Internet]. 2015. https://www.lagboken.se/Lagboken/start/miljoratt/miljobalk-1998808//d_2539466-sfs-2015_670-lag-om-andring-i-miljobalken.
 - [24] SFS 2015:216. Förordning om trafikbuller vid bostadsbyggnader [Ordinance on traffic noise near residential buildings] [Internet]. 2015. <https://www.riksdagen.se/sv/dokument-och-lagar/dokument/svensk-forfattningssamling/forordning-2015216-om-trafikbuller-vid-sfs-2015-216/>.
 - [25] Bravo-Moncayo L, Chávez M, Puyana V, Lucio-Naranjo J, Garzón C, Pavón-García I. A cost-effective approach to the evaluation of traffic noise exposure in the city of Quito, Ecuador. *Case Stud Transp Policy.* 2019;7(1):128–37. doi: 10.1016/j.cstp.2018.12.006.
 - [26] Melo RA, Pimentel RL, Lacerda DM, Silva WM. Applicability of models to estimate traffic noise for urban roads. *J Environ Health Sci Eng.* 2015;13(1):83. doi: 10.1186/s40201-015-0240-9.
 - [27] Stoter J, de Kluijver H, Kurakula V. 3D noise mapping in urban areas. *Geogr Inf Syst.* 2008;22(8):907–24. doi: 10.1080/13658810701739039.
 - [28] Swedish Association of Local Authorities and Regions (SALAR) [Sveriges Kommuner och Landsting]. Bygg bort bullret!: Bostadsbristen är växande hinder för städer och samhällen att utvecklas [Build out the noise!: The housing shortage is a growing obstacle preventing cities and communities to develop] [Internet]. 2013 [cited 2024 Nov 18]. <https://skr.se/download/18.3c9f9e1e17db3f33e522da5/1639429168021/5310.pdf>.
 - [29] Johansson O. Bullerregler som hindrar byggande (Interpellation 2020/21:522) [Noise regulations preventing construction] [Internet]. Riksdagen.se. 2020 [cited 2024 Nov 18]. https://www.riksdagen.se/sv/dokument-och-lagar/dokument/interpellation/bullerregler-som-hindrar-byggande_h810522.
 - [30] Arjunan A, Baroutaji A, Robinson J, Vance A, Arafat A. Acoustic metamaterials for sound absorption and insulation in buildings. *Build Environ.* 2024;251(111250):111250. doi: 10.1016/j.buildenv.2024.111250.
 - [31] De Salis MHF, Oldham DJ, Sharples S. Noise control strategies for naturally ventilated buildings. *Build Environ.* 2002;37(5):471–84. doi: 10.1016/s0360-1323(01)00047-6.
 - [32] Stoter J, Peters R, Commandeur T, Dukai B, Kumar K, Ledoux H. Automated reconstruction of 3D input data for noise simulation. *Comput Environ Urban Syst.* 2020;80(101424):101424. doi: 10.1016/j.compenvurbysys.2019.101424.
 - [33] Kephelopoulou S, Paviotti M, Anfosso-Lédée F, Van Maercke D, Shilton S, Jones N. Advances in the development of common noise assessment methods in Europe: The CNOSSOS-EU framework for strategic environmental noise mapping. *Sci Total Environ.* 2014;482–483:400–10. doi: 10.1016/j.scitotenv.2014.02.031.
 - [34] Kokkonen J, Kontkanen O, Majjala PP. CNOSSOS-EU noise model implementation in Finland In Baltic-Nordic Acoustic Meeting. 2016.
 - [35] Larsson K. Updated road traffic noise emission models in Sweden. In INTER-NOISE and NOISE-CON Congress and Conference Proceedings. 2016.
 - [36] Khan J, Ketzler M, Jensen SS, Gulliver J, Thysell E, Hertel O. Comparison of Road Traffic Noise prediction models: CNOSSOS-EU, Nord2000 and TRANEX. *Environ Pollut.* 2021;270(116240):116240. doi: 10.1016/j.envpol.2020.116240.

- [37] Khan J, Thysell E, Backalarz C, Finne P, Hertel O, Jensen SS. Performance evaluation of Nord2000, RTN-96 and CNOSSOS-EU against noise measurements in Central Jutland, Denmark. *Acoustics*. 2023;5(4):1099–122. doi: 10.3390/acoustics5040062.
- [38] Gustafson A, Genell A. Beräkning av vägtrafikbuller med CNOSSOS-EU, Nord2000 och Nord96 – En underlagsrapport, del 1 och 2. Gothenburg/Göteborg, Sweden/Sverige: Rapport för Kunskapscentrum om buller; 2022.
- [39] Kragh J, Jonasson H, Plovsing B, Sarinen A. User's Guide Nord2000 Road (AV 1171/06); 2006 [cited 2024 Nov 18]. <https://forcetechnology.com/-/media/force-technology-media/pdf-files/projects/nord2000/nord2000-users-guide-road.pdf>.
- [40] Naturvårdsverket. Nationella marktäckedata basskikt Skåne, Blekinge, Kronoberg, Halland, Kalmar, Jönköping, Östergötland, Örebro: Produktbeskrivning [Internet]. 2018 [cited 2024 Nov 18]. Available from: https://ext-dokument.lansstyrelsen.se//Ostergotland/Nationella%20Markt%C3%A4ckedata%20Produktbeskrivningar/NMD_Produktbeskrivning_Basskikt_regionA_v1.pdf.
- [41] Büttner G. CORINE land cover and land cover change products. In *Land use and land cover mapping in Europe: practices & trends*. Dordrecht: Springer Netherlands; 2014.
- [42] European Environmental Agency. EEA Geospatial Data Catalogue [Internet]. Urban Atlas Land Cover/Land Use 2012 (vector), Europe, 6-yearly; 2021 Jan [cited 2025 Jan 31]. <https://sdi.eea.europa.eu/catalogue/copernicus/api/records/debc1869-a4a2-4611-ae95-daeefce23490?language=all>.
- [43] Naturvårdsverket. Nationella marktäckedata 2018 tillägsskikt produktivitet: Produktbeskrivning [Internet]. 2023 [cited 2024 Nov 18]. https://geodata.naturvardsverket.se/nedladdning/marktacke/NMD2018/NMD_Produktbeskrivning_tillagsskikt_Produktivitet.pdf.
- [44] Belgii M, Dr Guł L, Strobl J. Quantitative evaluation of variations in rule-based classifications of land cover in urban neighbourhoods using WorldView-2 imagery. *ISPRS J Photogramm Remote Sens*. 2014;87(100):205–15. doi: 10.1016/j.isprsjprs.2013.11.007.
- [45] Yan WY, Shaker A, El-Ashmawy N. Urban land cover classification using airborne LiDAR data: A review. *Remote Sens Environ*. 2015;158:295–310. doi: 10.1016/j.rse.2014.11.001.
- [46] Sameen MI, Pradhan B, Aziz OS. Classification of very high resolution aerial photos using spectral-spatial convolutional neural networks. *J Sens*. 2018;2018:1–12. doi: 10.1155/2018/7195432.
- [47] Xu Z, Guan K, Casler N, Peng B, Wang S. A 3D convolutional neural network method for land cover classification using LiDAR and multi-temporal Landsat imagery. *ISPRS J Photogramm Remote Sens*. 2018;144:423–34. doi: 10.1016/j.isprsjprs.2018.08.005.
- [48] Stepchenko AM. Land-use classification using convolutional neural networks. *Autom Contr Comput Sci*. 2021;55(4):358–67. doi: 10.3103/s0146411621040088.
- [49] Dewangkoro HI, Arymurthy AM. Land use and land cover classification using CNN, SVM, and Channel Squeeze & Spatial Excitation block. *IOP Conf Ser Earth Environ Sci*. 2021;704(1):012048. doi: 10.1088/1755-1315/704/1/012048.
- [50] Fitton D, Laurens E, Hongkarnjanakul N, Schwob C, Mezeix L. Land cover classification through Convolutional Neural Network model assembly: A case study of a local rural area in Thailand. *Remote Sens Appl Soc Environ*. 2022;26(100740):100740. doi: 10.1016/j.rsase.2022.100740.
- [51] Hosseiny B, Abdi AM, Jamali S. Urban land use and land cover classification with interpretable machine learning – A case study using Sentinel-2 and auxiliary data. *Remote Sens Appl Soc Environ*. 2022;28(100843):100843. doi: 10.1016/j.rsase.2022.100843.
- [52] Cecili G, De Fioravante P, Dichico P, Congedo L, Marchetti M, Munafò M. Land cover mapping with convolutional neural networks using Sentinel-2 images: Case study of Rome. *Land (Basel)*. 2023;12(4):879. doi: 10.3390/land12040879.
- [53] Acuña-Alonso C, García-Ontiyuelo M, Barba-Barragáns D, Álvarez X. Development of a convolutional neural network to accurately detect land use and land cover. *MethodsX*. 2024;12(102719):102719. doi: 10.1016/j.mex.2024.102719.
- [54] Goodfellow I, Bengio Y, Courville A. *Deep learning*. Cambridge, Massachusetts, United States of America: MIT Press; 2016 [cited 2024 Nov 18]. <http://www.deeplearningbook.org>.
- [55] Rottensteiner F, Sohn G, Gerke M, Wegner JD. 2D Semantic Label. - Vaihingen. *ISPRS [Internet]*; 2013 [cited 2024 Nov 18]. <https://www.isprs.org/education/benchmarks/UrbanSemLab/2d-sem-label-vaihingen.aspx>.
- [56] Chiu MT, Xu X, Wei Y, Huang Z, Schwing AG, Brunner R, et al. Agriculture-vision: A large aerial image database for agricultural pattern analysis. In *2020 IEEE/CVF Conference on Computer Vision and Pattern Recognition (CVPR)*. IEEE; 2020. p. 2825–35.
- [57] NORDTEST. Ground surfaces: Determination of the acoustic impedance (NT ACOU 104) [Internet]. Espoo, Finland; 1999 [cited 2024 Nov 18]. <https://www.nordtest.info/wp/1999/11/01/617/>.
- [58] Sohlman M, Jonasson H, Gustafsson A. Using satellite data for the determination of the acoustic impedance of ground: Report to the Swedish National Space Board 2004-12. Swedish National Testing and Research Institute [Internet]. Diva-portal.org; 2004 [cited 2024 Nov 18]. <https://www.diva-portal.org/smash/get/diva2:1821327/FULLTEXT01.pdf>.
- [59] Hobbs CM, Gurovich YA, Boeker E, Hasting A, Rapoza A, Page J, et al. Improving AEDT noise modeling of mixed ground surfaces. Washington, D.C.: Transportation Research Board; 2017. doi: 10.17226/24822.
- [60] Gustafson A, Genell A, Ögren M. Rapporten innehåller metodstöd för beräkning av buller från väg- och spårtrafik med Nord2000 för svenskt bruk [Internet]; 2023 [cited 2024 Nov 18]. <http://kunskapscentrumbuller.se/documents/Anv%C3%A4ndarhandledning%20Nord2000%20version%200.9.pdf>.
- [61] Gustafson A, Genell A. NORD2000 – UNDERLAG TILL MARKIMPEDANS: Inventering av underlag för markimpedansklasser [Internet]. Kunskapscentrumbuller.se. 2024 [cited 2024 Nov 18]. <http://kunskapscentrumbuller.se/documents/Rapport%20inventering%20underlag%20f%C3%B6r%20markimpedans%20KCB%202024.pdf>.
- [62] Kolbe TH, Donaubaier A. Semantic 3D city modeling and BIM. In *The Urban Book Series*. Singapore: Springer Singapore; 2021. p. 609–36.
- [63] Gröger G, Kolbe TH, Nagel C, Häfele KH. OGC city geography markup language (CityGML) encoding standard (OGC 12-019) [Internet]. Open Geospatial Consortium; 2012 [cited 2024 Nov 18]. <http://www.opengis.net/spec/citygml/2.0>.
- [64] Kolbe TH, Kutzner T, Smyth CS, Nagel C, Roensdorf C, Heazel C. OGC City Geography Markup Language (CityGML) Part 1: Conceptual Model Standard, Ver. 3.0.0 [Internet]. Open Geospatial Consortium; 2022 May [cited 2024 Nov 18]. <http://www.opengeospatial.org/standards/citygml>.

- [65] Kumar K, Ledoux H, Commandeur TJF, Stoter JE. Modelling urban noise in CityGML Ade: Case of the Netherlands. *ISPRS Ann Photogramm Remote Sens Spat Inf Sci.* 2017;IV-4/W5:73–81. doi: 10.5194/isprs-annals-iv-4-w5-73-2017.
- [66] SoundPLAN GmbH. SoundPLANnoise 9.0: Manual [Internet]; 2023 [cited 2024 Nov 18]. https://www.soundplan.co.za/downloads/Documents/SoundPLAN_Noise_9.0_Manual.pdf.
- [67] Naturvårdsverket. Nationella marktäckedata 2018 teknisk rapport (1.0) [Internet]. 2019 [cited 2024 Nov 18]. <https://www.naturvardsverket.se/4ac30d/contentassets/37e8b38528774982b5840554f02a1f81/nmd-2018-teknisk-rapport.pdf>.
- [68] Chen L-C, Papandreou G, Schroff F, Adam H. Rethinking Atrous Convolution for Semantic Image Segmentation [Internet]. arXiv [cs.CV]; 2017. <http://arxiv.org/abs/1706.05587>.
- [69] He K, Zhang X, Ren S, Sun J. Deep residual learning for image recognition. In 2016 IEEE Conference on Computer Vision and Pattern Recognition (CVPR). IEEE; 2016. p. 770–8.
- [70] Ugglä M, Olsson P, Abdi B, Axelsson B, Calvert M, Christensen U, et al. Future Swedish 3D city models – specifications, test data, and evaluation. *ISPRS Int J Geoinf.* 2023;12(2):47. doi: 10.3390/ijgi12020047.
- [71] DataKustik GmbH. CadNAA CL Road [Internet]. DataKustik.com. 2024 [cited 2024 Nov 18]. <https://www.datakustik.com/noise-outdoors/road-and-railway-noise>.
- [72] Autodesk Inc. Spacemaker Software [Internet]. Autodesk.eu. 2024 [cited 2024 Nov 18]. <https://www.autodesk.eu/content/autodesk/global/en/products/spacemaker/overview.html>.
- [73] Biljecki F, Ledoux H, Stoter J. An improved LOD specification for 3D building models. *Comput Environ Urban Syst.* 2016;59:25–37. doi: 10.1016/j.compenvurbysys.2016.04.005.
- [74] Kephelopoulou S, Paviotti M, Anfosso-Lédée F. Common Noise Assessment Methods in Europe (CNOSSOS-EU). Luxembourg: JRC Publications Repository; 2012. doi: 10.2788/32029.
- [75] SoundPLAN. SoundPLAN – SoundPLAN GmbH [Internet]. SoundPLAN. 2024 [cited 2024 Nov 18]. <https://www.soundplan.eu/en/>.
- [76] Larsson K, Jonasson H. Uppdaterade beräkningsmodeller för vägtrafikbuller (2015:72). SP Sveriges Tekniska Forskningsinstitut [Internet]; 2015 [cited 2024 Nov 18]. <https://kunskapscentrumbuller.se/documents/Uppdaterade%20berakningsmodeller%20for%20vagtrafikbuller,%20K%20Larsson%20H%20Jonasson,%20SP%20Rapport%202015-72.pdf>.
- [77] Van Renterghem T, Botteldooren D. In-situ measurements of sound propagating over extensive green roofs. *Build Environ.* 2011;46(3):729–38. doi: 10.1016/j.buildenv.2010.10.006.
- [78] Kuras A, Brell M, Rizzi J, Burud I. Hyperspectral and lidar data applied to the urban land cover machine learning and neural-network-based classification: A review. *Remote Sens (Basel).* 2021;13(17):3393. doi: 10.3390/rs13173393.
- [79] Jäger D, Zellmann C, Schlatter F, Wunderli JM. Validation of the sonAIR aircraft noise simulation model. *Noise Mapp.* 2021;8(1):95–107. doi: 10.1515/noise-2021-0007.
- [80] SMHI. Ladda ner meteorologiska observationer | SMHI: Lufttemperatur (h): SMHIs stationsnät [Internet]. Smhi.se. 2024 [cited 2024 Nov 18]. <https://www.smhi.se/data/meteorologi/ladda-ner-meteorologiska-observationer/#param=airtemperatureInstant,stations=core,stationid=52350>.
- [81] SMHI. Ladda ner meteorologiska observationer | SMHI: Relativ luftfuktighet (h): SMHIs stationsnät [Internet]. Smhi.se. 2024 [cited 2024 Nov 18]. <https://www.smhi.se/data/meteorologi/ladda-ner-meteorologiska-observationer/#param=airHumidity,stations=core,stationid=52350>.
- [82] SMHI. Ladda ner meteorologiska observationer | SMHI: Vindriktning och vindhastighet (h): SMHIs stationsnät [Internet]. Smhi.se. 2024 [cited 2024 Nov 18]. <https://www.smhi.se/data/meteorologi/ladda-ner-meteorologiska-observationer/#param=wind,stations=core,stationid=52350>.
- [83] Liptai P, Badida M, Lukáčová K. Influence of atmospheric conditions on sound propagation - Mathematical modeling. *Phys Environ Sci.* 2015;5:1 [cited 2024 Nov 18], <https://api.semanticscholar.org/CorpusID:55807059>.
- [84] Khan J, Ketzel M, Kakosimos K, Sørensen M, Jensen SS. Road traffic air and noise pollution exposure assessment - A review of tools and techniques. *Sci Total Environ.* 2018;634:661–76. doi: 10.1016/j.scitotenv.2018.03.374.
- [85] Hadzi-Nikolova M, Mirakovski D, Ristova E, Stefanovska Ceravolo L. Modelling and Mapping of Urban Noise Pollution with SoundPLAN Software. *Int J Sci Tech Innov Ind MTM (Mach Technol Mater).* 2012;5:38–42.
- [86] Ögren M, Johansson H. Measurement of the acoustic impedance of ground (SP REPORT 1998:28). Borås, Sweden: Swedish National Testing and Research Institute; 1998 [cited 2024 Nov 18]. <http://www.diva-portal.se/smash/get/diva2:962071/FULLTEXT01.pdf>.

Appendix

A1 National specifications for land cover

Currently, *Lantmäteriet* is in the process of reviewing the National Specifications for Land Cover (NS-LC). The tables below, present an example of one of the latest suggestions (as of June 2023). The NS-LC organizes LC into six main thematic classes; *forestland*, *open wetlands*, *open solid ground*, *bare mountainous areas* (tundra), *built-up surfaces*, and *water*. As different applications utilizing LC might have different requirements regarding the level of detail (LOD), this information is presented at four LODs; L1-L4 (with L4 representing the highest LOD). The ambition of this reviewing work is to implement one common national LC classification that meets the demands of all main applications where LC is used. The tables below present LC information at four LODs for the thematic classes present in the study area: *built-up surfaces*, *open solid ground*, and *water*.

A2 Noise impedance values per NS-LC thematic class

This section presents a table with the flow resistivity value associated with every NS-LC thematic class. Table A4 also includes a column for grouping the NS-LC thematic classes into hard or soft surfaces. A short description justifying the selection of flow resistivity value per NS-LC thematic class is also provided.

A3 NMD LC to NS-LC conversion table

This section presents the conversion table (Table A5) used to convert NMD LC thematic classes to NS-LC thematic

classes. It should be noted that though NS-LC for *forests* are based on NMD LC for *forests* and have identical names in both LC classification systems, we took a different approach in our study differentiating on-ground from above-ground vegetation. This was done because in noise simulations we are more interested in the acoustic properties of the ground surface material. Above-ground vegetation can be represented by 3D vegetation objects as described in the CityGML vegetation theme [63]. Therefore, all forest-related NMD LCs have been transformed to NS-LC “*Open solid ground; Vegetated ground*.” No NMD LC class for *forest on wetlands* was detected in our study area. More research is needed to map the *forest on wetland* NMD LC classes to a ground surface equivalent in NS-LC.

A4 NMD examples of hard surface areas classified as vegetation

This section is dedicated to presenting examples of surfaces that have mistakenly been classified as vegetation by the NMD algorithm. The examples include screenshots from Google Earth and Google Street View of the areas in question.

Figure A1 shows an example of how rich foliage on trees with wide tree crowns can hide the true ground surface and lead to erroneous LC classifications in NMD.

Figures A2 and A3 present an example of a case when vegetation on balconies and green roofs of buildings with a complex typology can lead the NMD algorithm to misinterpret the ground surface for *forest* instead of *building*.

Figures A4 and A5 depict examples of climbing plants on building facades and external walls that have been erroneously classified as *forest* or *vegetation*.

Table A1: Levels of detail for LC classes of the theme *built-up surfaces*

LC theme	Level 2 (L2)	Level 3 (L3)	Level 4 (L4)	Example
Built-up surfaces	Building surfaces	Building surfaces	Building surfaces	
				
	Road and railway surfaces	Road and railway surfaces	Road and railway surfaces	
				

(Continued)

Table A1: Continued

LC theme	Level 2 (L2)	Level 3 (L3)	Level 4 (L4)	Example
	Other built-up surfaces	Other built-up surfaces – hard ground	Other built-up surfaces – hard ground – paving stone	
			Other built-up surfaces – hard ground – cobblestone	
			Other built-up surfaces – hard ground – asphalt	 

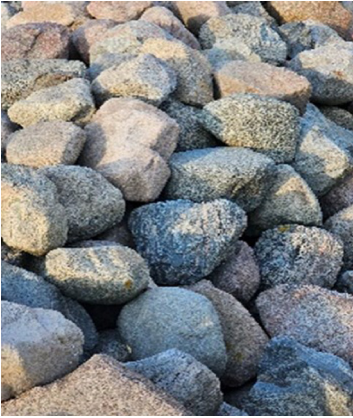


(Continued)

Table A1: Continued

LC theme	Level 2 (L2)	Level 3 (L3)	Level 4 (L4)	Example
			Other built-up surfaces – hard ground – stone tiles	
			Other built-up surfaces – hard ground – concrete	
			Other built-up surfaces – hard ground –gravel	

(Continued)

Table A1: Continued

LC theme	Level 2 (L2)	Level 3 (L3)	Level 4 (L4)	Example
			Other built-up surfaces – hard ground – natural stone	
			Other built-up surfaces – hard ground – artificial grass	
			Other built-up surfaces – hard ground – rubber coating	

(Continued)

Table A1: *Continued*



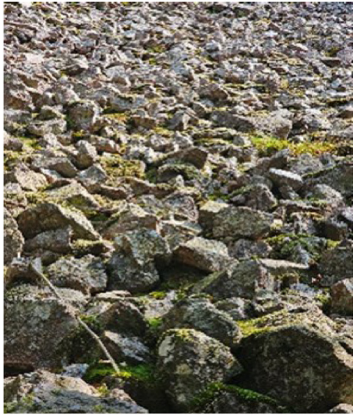
LC theme	Level 2 (L2)	Level 3 (L3)	Level 4 (L4)	Example
		Other built-up surfaces – excavated ground	Other built-up surfaces – excavated ground	

Table A2: Levels of detail for LC classes of theme *open solid ground*

LC theme	Level 2 (L2)	Level 3 (L3)	Level 4 (L4)	Example
Open solid ground	Bare ground	Bare ground – mountains	Bare ground – mountains	
		Bare ground – loose soil types	Bare ground – loose soil types – boulder/rocks	





(Continued)

Table A2: Continued

LC theme	Level 2 (L2)	Level 3 (L3)	Level 4 (L4)	Example
			Bare ground – loose soil types – gravel soil	
			Bare ground – loose soil types – sandy ground	
			Bare ground – loose soil types – marl	


(Continued)

Table A2: *Continued*

LC theme	Level 2 (L2)	Level 3 (L3)	Level 4 (L4)	Example
				
	Vegetated ground	Vegetated ground – low vegetation – grassland	Vegetated ground – low vegetation – grassland – dry	
			Vegetated ground – low vegetation – grassland – healthy	
			Vegetated ground – low vegetation – grassland – moist	

(Continued)

Table A2: Continued

LC theme	Level 2 (L2)	Level 3 (L3)	Level 4 (L4)	Example
		Vegetated ground – low vegetation – paddy-field	Vegetated ground – low vegetation – paddy-field – dry	
			Vegetated ground – low vegetation – paddy-field – healthy	
			Vegetated ground – low vegetation – paddy-field – moist	
	Vegetated ground – low vegetation – shrubland		Vegetated ground – low vegetation – shrubland – coniferous shrublands	

(Continued)

Table A2: *Continued*



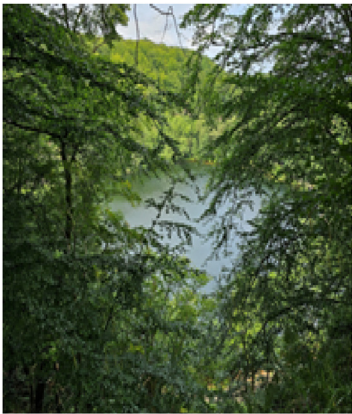



LC theme	Level 2 (L2)	Level 3 (L3)	Level 4 (L4)	Example
			Vegetated ground – low vegetation – shrubland – leaf shrublands	

Table A3: Levels of detail for LC classes of theme *water*

LC theme	Level 2 (L2)	Level 3 (L3)	Example
Water	Sea	Sea	
	Lake	Lake	

(Continued)

Table A3: Continued

LC theme	Level 2 (L2)	Level 3 (L3)	Example
	Manmade still water facilities	Manmade still water facilities – reservoir Manmade still water facilities – dam	
		Manmade still water facilities – pool	
	Stream	Stream	
	Manmade running water facilities	Manmade running water facilities – canal	

(Continued)

Table A3: *Continued*


LC theme	Level 2 (L2)	Level 3 (L3)	Example
		Manmade running water facilities – ditch	

Table A4: Grouping of NS-LC thematic classes to hard/soft surfaces

NS-LC thematic class	“Hard” or “Soft” surface	Flow resistivity value σ (kPa s/m ²)
Built-up surfaces; Other built-up surfaces; Hard ground; Asphalt*	Hard	20,000
Built-up surfaces; Other built-up surfaces; Hard ground; Concrete*	Hard	200,000
Built-up surfaces; Other built-up surfaces; Hard ground; Paving stone**	Hard	2,000
Built-up surfaces; Other built-up surfaces; Hard ground; Rubber coating**	Hard	500
Built-up surfaces; Other built-up surfaces; Hard ground; Artificial grass**	Hard	500
Built-up surfaces; Other built-up surfaces; Hard ground; Cobblestone**	Hard	2,000
Built-up surfaces; Other built-up surfaces; Hard ground; Stone tiles**	Hard	2,000
Built-up surfaces; Other built-up surfaces; Hard ground; Natural stone**	Hard	2,000
Built-up surfaces; Other built-up surfaces; Hard ground; Gravel*	Hard	2,000
Built-up surfaces; Other built-up surfaces; Excavated ground; Excavated ground*	Soft	80
Built-up surfaces; Building surfaces; Building surfaces; Building surfaces***	Hard	500
Built-up surfaces; Road and railway surfaces; Road and railway surfaces; Road and railway surfaces**	Hard	20,000
Water; Manmade still water facilities; Pool**	Hard	20,000
Water; Manmade still water facilities; Dam**	Hard	20,000
Open solid ground; Vegetated ground; Low vegetation; Shrubland**	Soft	80
Open solid ground; Vegetated ground; Low vegetation; Grassland**	Soft	200
Broad-leaved deciduous forest (outside wetlands)**	Soft	32
Built-up surfaces; Other built-up surfaces**	Hard	2,000
Mixed broad-leaved deciduous and coniferous forest (outside wetlands)**	Soft	80
Open solid ground; Vegetated ground**	Soft	500
Coniferous forest (outside wetlands)**	Soft	80
Trivial deciduous forest (outside wetlands)**	Soft	32
Trivial deciduous and broad-leaved deciduous forest (outside wetlands)**	Soft	32

The annotated text corresponds to the NS-LC thematic classes of the NMD NS-LC automatic layer.

* = Flow resistivity values are derived from Table 10 “Classification of ground type” in [39].

** = Flow resistivity values for different types of forests, urban green areas, forest bush/transition stage areas, water, and missing LC class (relevant for the LC classes *rubber coating* and *artificial grass*) were derived from Table 5.5 of a technical report to the Swedish National Space Board by (2004-12) titled “Using Satellite data for the determination of the acoustic impedance of ground” by Sohlman *et al.* [58]. Flow resistivity values for lawn (not trodden on) were derived from documentation on page 37 of Sohlman *et al.* [58]. The flow resistivity value for roads (not railways in this case) is derived from Table 5.4 (normal paved road) in Sohlman *et al.* [58]. The flow resistivity value for built-up areas (*i.e.* Built-up surfaces; Other built-up surfaces) is derived from Table 5.3 (compacted dense ground) in Sohlman *et al.* [58]. The flow resistivity value assigned to built-up LC classes including some type of stone (*e.g.* paving stone (*gatsten*), cobblestone (*kullersten*), stone tiles (*marksten*), natural stone (*natursten*)) was derived from the content of page 37 of Sohlman *et al.* [58] and from Table 8.1 in the technical report by Ögren and Johansson [86].

*** = Flow resistivity values are derived from Table 2 “Impedance class for the land cover types included in the Swedish National Mapping Agency’s property map” in Gustafson *et al.* [60].

Table A5: NMD LC to NS-LC conversion table

Thematic LC classes NMD	NMD code	Thematic LC classes NS-LC	Notes
Pine forest (outside wetlands)	111	Pine forest (outside wetlands)	Replaced by NS-LC (L2): Open solid ground; Vegetated ground
Spruce forest (outside wetlands)	112	Spruce forest (outside wetlands)	Replaced by NS-LC (L2): Open solid ground; Vegetated ground
Coniferous mixed forest (outside wetlands)	113	Coniferous mixed forest (outside wetlands)	Replaced by NS-LC (L2): Open solid ground; Vegetated ground
Mixed deciduous coniferous forest (outside wetlands)	114	Mixed deciduous coniferous forest (outside wetlands)	Replaced by NS-LC (L2): Open solid ground; Vegetated ground
Trivial deciduous forest (outside wetlands)	115	Trivial deciduous forest (outside wetlands)	Replaced by NS-LC (L2): Open solid ground; Vegetated ground
Broad-leaved deciduous forest (outside wetlands)	116	Broad-leaved deciduous forest (outside wetlands)	Replaced by NS-LC (L2): Open solid ground; Vegetated ground
Trivial deciduous and broad-leaved deciduous forest (outside wetlands)	117	Trivial deciduous and broad-leaved deciduous forest (outside wetlands)	Replaced by NS-LC (L2): Open solid ground; Vegetated ground
Temporarily no forest (outside wetlands)	118	Temporarily no forest (outside wetlands)	Replaced by NS-LC (L2): Open solid ground; Vegetated ground
Pine forest (on wetland)	121	Pine forest (on wetland)	NS-LC follows NMD-LC classification for forest. No forest on wetland was included in our study.
Spruce forest (on wetland)	122	Spruce forest (on wetland)	NS-LC follows NMD-LC classification for forest. No forest on wetland was included in our study
Coniferous mixed forest (on wetland)	123	Coniferous mixed forest (on wetland)	NS-LC follows NMD-LC classification for forest. No forest on wetland was included in our study.
Mixed deciduous coniferous forest (on wetland)	124	Mixed deciduous coniferous forest (on wetland)	NS-LC follows NMD-LC classification for forest. No forest on wetland was included in our study
Trivial deciduous forest (on wetland)	125	Trivial deciduous forest (on wetland)	NS-LC follows NMD-LC classification for forest. No forest on wetland was included in our study.
Broad-leaved deciduous forest (on wetland)	126	Broad-leaved deciduous forest (on wetland)	NS-LC follows NMD-LC classification for forest. No forest on wetland was included in our study
Trivial deciduous and broad-leaved deciduous forest (on wetland)	127	Trivial deciduous and broad-leaved deciduous forest (on wetland)	NS-LC follows NMD-LC classification for forest. No forest on wetland was included in our study
Temporarily no forest (on wetland)	128	Temporarily no forest (on wetland)	NS-LC follows NMD-LC classification for forest. No forest on wetland was included in our study
Open wetland	2	Open wetland	
Arable land	3	Open solid ground; Vegetated ground; Low vegetation; Grassland	
Other open land without vegetation	41	Built-up surfaces; Other built-up surfaces	
Other open land with vegetation	42	Open solid ground; Vegetated ground; Low vegetation	
Exploited land, building	51	Built-up surfaces; Building surfaces; Building surfaces; Building surfaces	
Exploited land, not building or road/railway	52	Built-up surfaces; Other built-up surfaces	
Exploited land, road/railway	53	Built-up surfaces; Road and railway surfaces; Road and railway surfaces; Road and railway surfaces	
Lake and watercourse/stream	61	Water; Lake; Lake	
Sea	62	Water; Sea; Sea	



Figure A1: Screenshots over Vilebovägen 19A, 217 63 Malmö, Sweden showing how an NMD raster cell (left photo) has been classified as forest, when it in fact is asphalt (walking path).



Figure A2: Screenshots over Stensjögatan 66, 217 65 Malmö, Sweden showing how a NMD raster cell (left photo) has wrongfully been classified as forest, when it is a building.



Figure A3: Screenshots over Vilebovägen 25, 217 63 Malmö, Sweden showing how a NMD raster cell (left photo) has wrongfully been classified as *forest*, when it is a building with a green roof.



Figure A4: Screenshots over Eric Perssons väg 1, 217 62 Malmö, Sweden showing how an NMD raster cell (left photo) has wrongfully been classified as *forest*, when it is a building façade with climbing plants.



Figure A5: Screenshots over Vändåkersvägen 21, Malmö, Sweden showing how a NMD raster cell (left photo) has wrongfully been classified as *forest*, when it is a building façade with climbing plants.